16. T. Conrad, A. Akhtar, *Nat. Rev. Genet.* **13**, 123–134 (2011).
17. A. A. Alekseyenko *et al.*, *Cell* **134**, 599–609 (2008).
18. A. A. Alekseyenko *et al.*, *Genes Dev.* **27**, 853–858 (2013).
19. I. Marín, A. Franke, G. J. Bashaw, B. S. Baker, *Nature* **383**, 160–163 (1996).
20. Materials and methods are available as supplementary materials on *Science* Online.
21. Q. Zhou, C. E. Ellison, V. B. Kaiser, A. A. Alekseyenko, A. A. Gorchakov, D. Bachtrog, *PLoS Biol.* **11**, e1001711 (2013).
22. M. Steinemann, S. Steinemann, *Proc. Natl. Acad. Sci. U.S.A.* **89**, 7591–7595 (1992).
23. J. Jurka, *Repbase Reports* **12**, 1376 (2012).
24. V. V. Kapitonov, J. Jurka, *Trends Genet.* **23**, 521–529 (2007).
25. J. R. Bateman, A. M. Lee, C. T. Wu, *Genetics* **173**, 769–777 (2006).
26. Q. Zhou, D. Bachtrog, *Science* **337**, 341–345 (2012).
27. C. E. Grant, T. L. Bailey, W. S. Noble, *Bioinformatics* **27**, 1017–1018 (2011).

Acknowledgments: This work was funded by NIH grants (R01GM076007 and R01GM093182) and a Packard Fellowship to D.B. and a NIH postdoctoral fellowship to C.E.E. All DNA-sequencing reads generated in this study are deposited at the National Center for Biotechnology Information Short Reads Archive (www.ncbi.nlm.nih.gov/sra) under the accession no. SRS402821. The genome assemblies are available at the National Center for Biotechnology Information under BioProject PRJNA77213. We thank Z. Walton and A. Gorchakov for technical assistance.

Supplementary Materials

www.sciencemag.org/content/342/6160/846/suppl/DC1
Materials and Methods
Supplementary Text
Figs. S1 to S20
Tables S1 to S3
References (*28*–*54*)

23 April 2013; accepted 30 September 2013
10.1126/science.1239552

High-Resolution Global Maps of 21st-Century Forest Cover Change

M. C. Hansen,[1]* P. V. Potapov,[1] R. Moore,[2] M. Hancher,[2] S. A. Turubanova,[1] A. Tyukavina,[1] D. Thau,[2] S. V. Stehman,[3] S. J. Goetz,[4] T. R. Loveland,[5] A. Kommareddy,[6] A. Egorov,[6] L. Chini,[1] C. O. Justice,[1] J. R. G. Townshend[1]

Quantification of global forest change has been lacking despite the recognized importance of forest ecosystem services. In this study, Earth observation satellite data were used to map global forest loss (2.3 million square kilometers) and gain (0.8 million square kilometers) from 2000 to 2012 at a spatial resolution of 30 meters. The tropics were the only climate domain to exhibit a trend, with forest loss increasing by 2101 square kilometers per year. Brazil's well-documented reduction in deforestation was offset by increasing forest loss in Indonesia, Malaysia, Paraguay, Bolivia, Zambia, Angola, and elsewhere. Intensive forestry practiced within subtropical forests resulted in the highest rates of forest change globally. Boreal forest loss due largely to fire and forestry was second to that in the tropics in absolute and proportional terms. These results depict a globally consistent and locally relevant record of forest change.

Changes in forest cover affect the delivery of important ecosystem services, including biodiversity richness, climate regulation, carbon storage, and water supplies (*1*). However, spatially and temporally detailed information on global-scale forest change does not exist; previous efforts have been either sample-based or employed coarse spatial resolution data (*2*–*4*). We mapped global tree cover extent, loss, and gain for the period from 2000 to 2012 at a spatial resolution of 30 m, with loss allocated annually. Our global analysis, based on Landsat data, improves on existing knowledge of global forest extent and change by (i) being spatially explicit; (ii) quantifying gross forest loss and gain; (iii) providing annual loss information and quantifying trends in forest loss; and (iv) being derived through an internally consistent approach that is exempt from the vagaries of different definitions, methods, and data inputs. Forest loss was defined as a stand-replacement disturbance or the complete removal of tree cover canopy at the Landsat pixel scale. Forest gain was defined as the inverse of loss, or the establishment of tree canopy from a nonforest state. A total of 2.3 million km^2 of forest were lost due to disturbance over the study period and 0.8 million km^2 of new forest established. Of the total area of combined loss and gain (2.3 million km^2 + 0.8 million km^2), 0.2 million km^2 of land experienced both loss and subsequent gain in forest cover during the study period. Global forest loss and gain were related to tree cover density for global climate domains, ecozones, and countries (refer to tables S1 to S3 for all data references and comparisons). Results are depicted in Fig. 1 and are viewable at full resolution at http://earthenginepartners.appspot.com/science-2013-global-forest.

The tropical domain experienced the greatest total forest loss and gain of the four climate domains (tropical, subtropical, temperate, and boreal), as well as the highest ratio of loss to gain (3.6 for >50% of tree cover), indicating the prevalence of deforestation dynamics. The tropics were the only domain to exhibit a statistically significant trend in annual forest loss, with an estimated increase in loss of 2101 km^2/year. Tropical rainforest ecozones totaled 32% of global forest cover loss, nearly half of which occurred in South American rainforests. The tropical dry forests of South America had the highest rate of tropical forest loss, due to deforestation dynamics in the Chaco woodlands of Argentina, Paraguay (Fig. 2A), and Bolivia. Eurasian rainforests (Fig. 2B) and dense tropical dry forests of Africa and Eurasia also had high rates of loss.

Recently reported reductions in Brazilian rainforest clearing over the past decade (*5*) were confirmed, as annual forest loss decreased on average 1318 km^2/year. However, increased annual loss of Eurasian tropical rainforest (1392 km^2/year), African tropical moist deciduous forest (536 km^2/year), South American dry tropical forest (459 km^2/year), and Eurasian tropical moist deciduous (221 km^2/year) and dry (123 km^2/year) forests more than offset the slowing of Brazilian deforestation. Of all countries globally, Brazil exhibited the largest decline in annual forest loss, with a high of over 40,000 km^2/year in 2003 to 2004 and a low of under 20,000 km^2/year in 2010 to 2011. Of all countries globally, Indonesia exhibited the largest increase in forest loss (1021 km^2/year), with a low of under 10,000 km^2/year from 2000 through 2003 and a high of over 20,000 km^2/year in 2011 to 2012. The converging rates of forest disturbance of Indonesia and Brazil are shown in Fig. 3. Although the short-term decline of Brazilian deforestation is well documented, changing legal frameworks governing Brazilian forests could reverse this trend (*6*). The effectiveness of Indonesia's recently instituted moratorium on new licensing of concessions in primary natural forest and peatlands (*7*), initiated in 2011, is to be determined.

Subtropical forests experience extensive forestry land uses where forests are often treated as a crop and the presence of long-lived natural forests is comparatively rare (*8*). As a result, the highest proportional losses of forest cover and the lowest ratio of loss to gain (1.2 for >50% of tree cover) occurred in the subtropical climate domain. Aggregate forest change, or the proportion of total forest loss and gain relative to year-2000 forest area [(loss+gain)/2000 forest], equaled 16%, or more than 1% per year across all forests within the domain. Of the 10 subtropical humid and dry forest ecozones, 5 have aggregate forest change >20%, three >10%, and two >5%. North American subtropical forests of the southeastern United States are unique in terms of change dynamics because of short-cycle tree planting and harvesting (Fig. 2C). The disturbance rate of this ecozone was four times that of South American

[1]Department of Geographical Sciences, University of Maryland, College Park, MD 20742, USA. [2]Google, Mountain View, CA, USA. [3]Department of Forest and Natural Resources Management, State University of New York, Syracuse, NY, USA. [4]Woods Hole Research Center, 149 Woods Hole Road, Falmouth, MA 02540, USA. [5]Earth Resources Observation and Science, United States Geological Survey, 47914 252nd Street, Sioux Falls, SD 57198, USA. [6]Geographic Information Science Center of Excellence, South Dakota State University, Brookings, SD, USA.

*Corresponding author. E-mail: mhansen@umd.edu

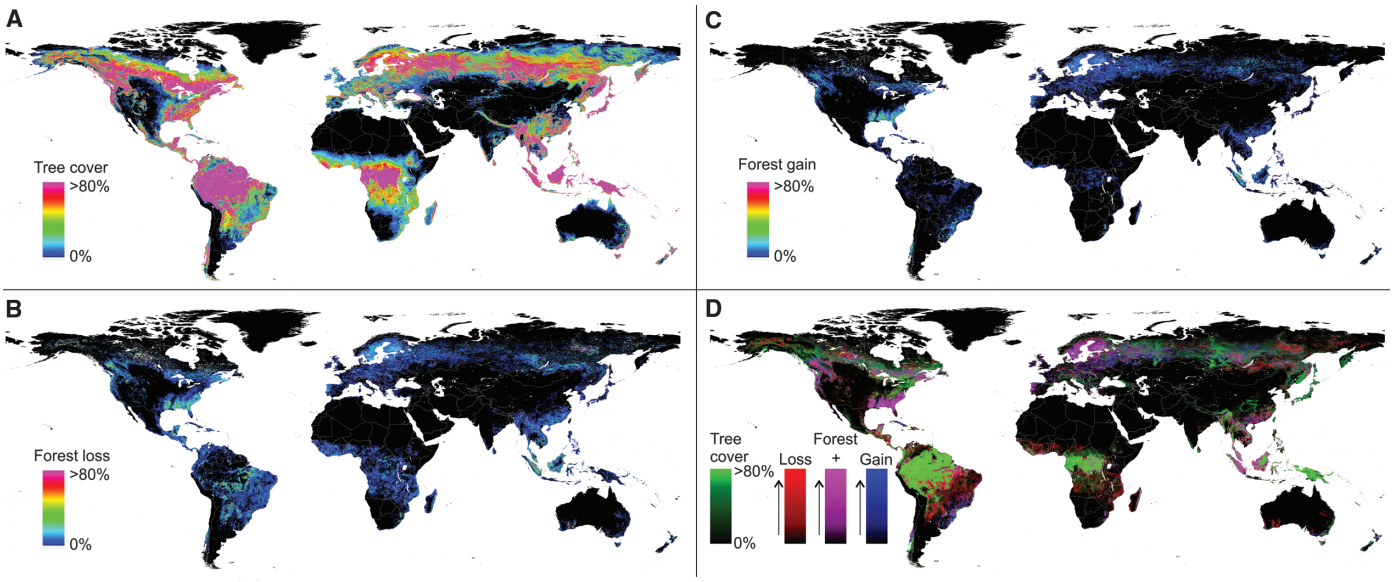

Fig. 1. (A) Tree cover, (B) forest loss, and (C) forest gain. A color composite of tree cover in green, forest loss in red, forest gain in blue, and forest loss and gain in magenta is shown in (**D**), with loss and gain enhanced for improved visualization. All map layers have been resampled for display purposes from the 30-m observation scale to a 0.05° geographic grid.

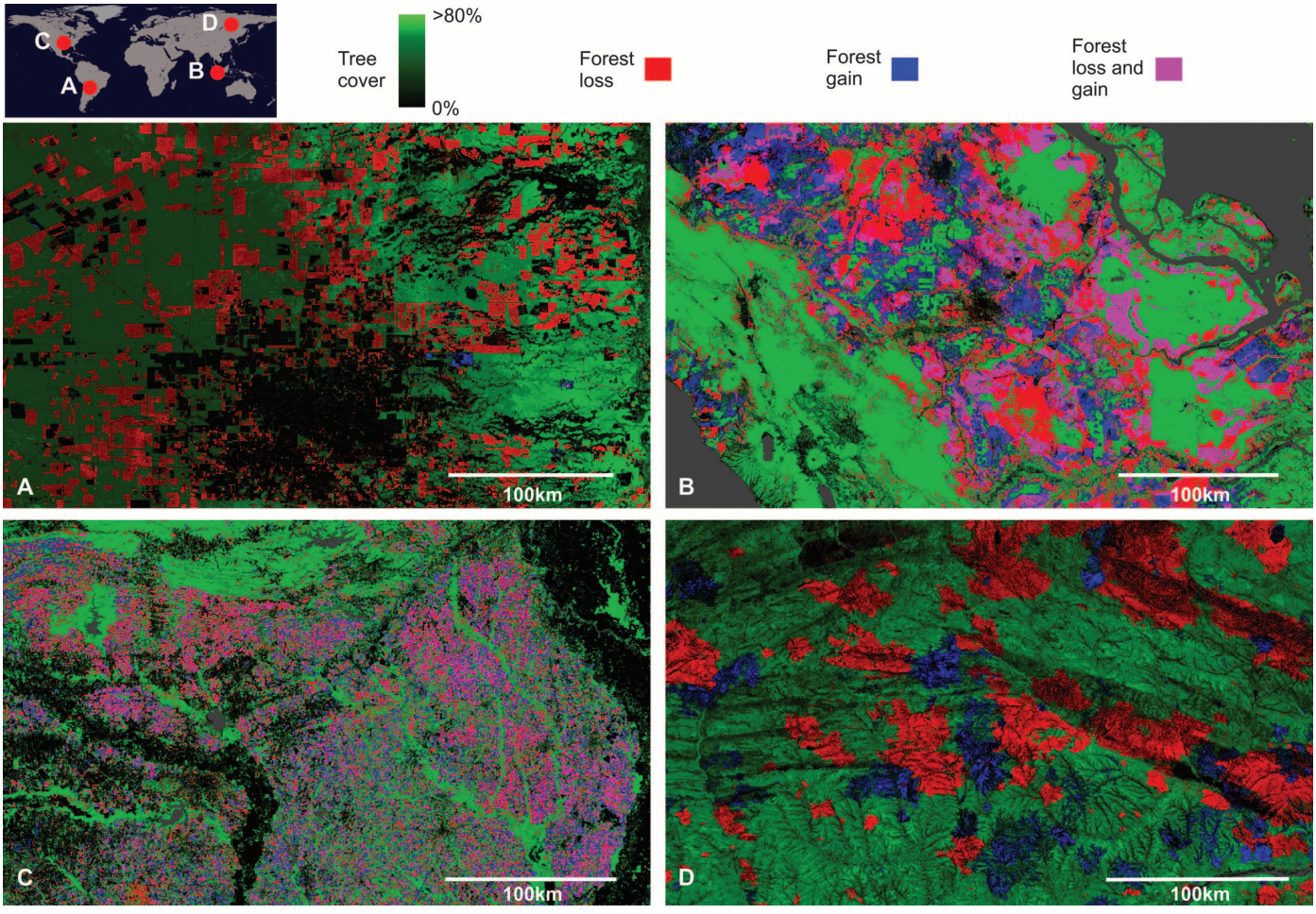

Fig. 2. Regional subsets of 2000 tree cover and 2000 to 2012 forest loss and gain. (**A**) Paraguay, centered at 21.9°S, 59.8°W; (**B**) Indonesia, centered at 0.4°S, 101.5°E; (**C**) the United States, centered at 33.8°N, 93.3°W; and (**D**) Russia, centered at 62.1°N, 123.4°E.

rainforests during the study period; over 31% of its forest cover was either lost or regrown. Areas of colocated loss and gain (magenta tones in Fig. 1D), indicating intensive forestry practices, are found on all continents within the subtropical climate domain, including South Africa, central Chile, southeastern Brazil, Uruguay, southern China, Australia, and New Zealand.

The temperate climatic domain has a forestry-dominant change dynamic and a relatively low ratio of loss to gain (1.6 for >50% of tree cover). Oceanic ecozones, in particular, are similar to the subtropics in the intensity of indicated forest land use. The northwest United States is an area of intensive forestry, as is the entire range of temperate Canada. The intermountain West of North America exhibits a loss dynamic, largely due to fire, logging, and disease [for example, large-scale tree mortality due to mountain pine bark beetle infestation, most evident in British Colombia, Canada (*9*)]. Temperate Europe has a forestry dynamic with Estonia and Latvia exhibiting a high ratio of loss to gain. Portugal, which straddles the temperate and subtropical domains, has a complicated dynamic of forestry and forest loss due to fire; the resulting aggregate change dynamic is fourth in intensity globally. Elevated loss due to storm damage is indicated for a few areas. For example, a 2005 extratropical cyclone led to a historic blowdown of southern Sweden temperate forests, and a 2009 windstorm leveled extensive forest areas in southwestern France (*10*).

Fire is the most significant cause of forest loss in boreal forests (*11*), and it occurred across a range of tree canopy densities. Given slower regrowth dynamics, the ratio of boreal forest loss to gain is high over the study period (2.1 for >50% of tree cover). Boreal coniferous and mountain ecozones are similar in terms of forest loss rates, with North America having a higher overall rate and Eurasia a higher absolute area of loss. Forest gain is substantial in the boreal zone, with Eurasian coniferous forests having the largest area of gain of all global ecozones during the study period, due to forestry, agricultural abandonment (*12*), and forest recovery after fire [as in European Russia and the Siberia region of Russia (Fig. 2D)]. Russia has the most forest loss globally. Co-located gain and loss are nearly absent in the high-latitude forests of the boreal domain, reflecting a slower regrowth dynamic in this climatic domain. Areas with loss and gain in close proximity, indicating forestry land uses, are found within nearly the entirety of Sweden and Finland, the boreal/temperate transition zone in eastern Canada, parts of European Russia, and along the Angara River in central Siberia, Russia.

A goal of large-area land cover mapping is to produce globally consistent characterizations that have local relevance and utility; that is, reliable information across scales. Figure S1 reflects this capability at the national scale. Two measures of change, (i) proportion of total aggregate forest change relative to year-2000 forest area [(loss + gain)/2000 forest], shown in column q of table S3; and (ii) proportion of total change that is loss [loss/(loss + gain)], calculated from columns b and c in table S3, are displayed. The proportion of total aggregate forest change emphasizes countries with likely forestry practices by including both loss and gain in its calculation, whereas the proportion of loss to gain measure differentiates countries experiencing deforestation or another loss dynamic without a corresponding forest recovery signal. The two ratio measures normalize the forest dynamic in order to directly compare national-scale change regardless of country size or absolute area of change dynamic. In fig. S1, countries that have lost forests without gain are high on the *y* axis (Paraguay, Mongolia, and Zambia). Countries with a large fraction of forest area disturbed and/or reforested/afforested are high on the *x* axis (Swaziland, South Africa, and Uruguay). Thirty-one countries have an aggregate dynamic >1% per year, 11 have annual loss rates >1%, and 5 have annual gain rates of >1%. Figure S2 compares forest change dynamics disaggregated by ecozone (http://foris.fao.org/static/data/fra2010/ecozones2010.jpg).

Brazil is a global exception in terms of forest change, with a dramatic policy-driven reduction in Amazon Basin deforestation. Although Brazilian gross forest loss is the second highest globally, other countries, including Malaysia, Cambodia, Cote d'Ivoire, Tanzania, Argentina, and Paraguay, experienced a greater percentage of loss of forest cover. Given consensus on the value of natural forests to the Earth system, Brazil's policy intervention is an example of how awareness of forest valuation can reverse decades of previous widespread deforestation. International policy initiatives, such as the United Natons Framework Convention of Climate Change Reducing Emissions from Deforestation and forest Degradation (REDD) program (*13*), often lack the institutional investment and scientific capacity to begin implementation of a program that can make use of the global observational record; in other words, the policy is far ahead of operational capabilities (*14*). Brazil's use of Landsat data in documenting trends in deforestation was crucial to its policy formulation and implementation. To date, only Brazil produces and shares spatially explicit information on annual forest extent and change. The maps and statistics we present can be used as an initial reference for a number of countries lacking such data, as a spur to capacity building in the establishment of national-scale forest extent and change maps, and as a basis of comparison in evolving national monitoring methods.

Global-scale studies require systematic global image acquisitions available at low or no direct

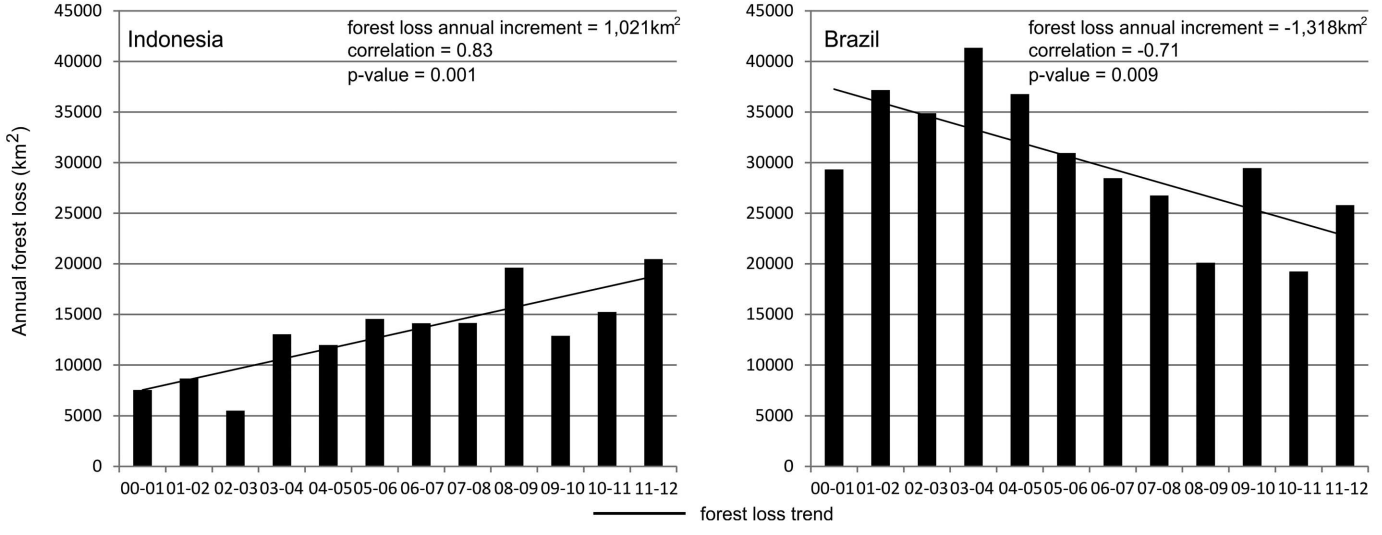

Fig. 3. Annual forest loss totals for Brazil and Indonesia from 2000 to 2012. The forest loss annual increment is the slope of the estimated trend line of change in annual forest loss.

cost and the preprocessing of geometric and radiometric corrections of satellite imagery, exemplified by the Landsat program. Given such progressive data policies and image processing capabilities, it is now possible to use advanced computing systems, such as the Google cloud, to efficiently process and characterize global-scale time-series data sets in quantifying land change. There are several satellite systems in place or planned for collecting data with similar capabilities to Landsat. Similar free and open data policies would enable greater use of these data for public good and foster greater transparency of the development, implementation, and reactions to policy initiatives that affect the world's forests.

The information content of the presented data sets, which are publicly available, provides a transparent, sound, and consistent basis on which to quantify critical environmental issues, including (i) the proximate causes of the mapped forest disturbances (*15*); (ii) the carbon stocks and associated emissions of disturbed forest areas (*16*–*18*); (iii) the rates of growth and associated carbon stock gains for both managed and unmanaged forests (*19*); (iv) the status of remaining intact natural forests of the world and threats to biodiversity (*20*, *21*); (v) the effectiveness of existing protected-area networks (*22*); (vi) the economic drivers of natural forest conversion to more intensive land uses (*23*); (vii) the relationships between forest dynamics and social welfare, health, and other relevant human dimensions data; (viii) forest dynamics associated with governance and policy actions—and many other regional-to-global–scale applications.

References and Notes

1. J. A. Foley *et al.*, *Science* **309**, 570–574 (2005).
2. M. C. Hansen, S. V. Stehman, P. V. Potapov, *Proc. Natl. Acad. Sci. U.S.A.* **107**, 8650–8655 (2010).
3. Food and Agricultural Organization of the United Nations, *Global Forest Land-Use Change 1990-2005, FAO Forestry Paper No. 169* (Food and Agricultural Organization of the United Nations, Rome, 2012).
4. M. Hansen, R. DeFries, *Ecosystems* **7**, 695–716 (2004).
5. Instituto Nacional de Pesquisas Especias, *Monitoring of the Brazilian Amazonian Forest by Satellite, 2000-2012* (Instituto Nacional de Pesquisas Especias, San Jose dos Campos, Brazil, 2013).
6. G. Sparovek, G. Berndes, A. G. O. P. Barretto, I. L. F. Klug, *Environ. Sci. Policy* **16**, 65–72 (2012).
7. D. P. Edwards, W. F. Laurance, *Nature* **477**, 33 (2011).
8. M. Drummond, T. Loveland, *Bioscience* **60**, 286–298 (2010).
9. W. A. Kurz *et al.*, *Nature* **452**, 987–990 (2008).
10. B. Gardiner *et al.*, *Destructive Storms in European Forests: Past and Forthcoming Impacts* (European Forest Institute, Freiburg, Germany, 2010).
11. P. Potapov, M. Hansen, S. Stehman, T. Loveland, K. Pittman, *Remote Sens. Environ.* **112**, 3708–3719 (2008).
12. A. Prishchepov, D. Muller, M. Dubinin, M. Baumann, V. Radeloff, *Land Use Policy* **30**, 873–884 (2013).
13. United Nations Framework Convention on Climate Change, *Reducing Emissions from Deforestation in Developing Countries: Approaches to Stimulate Action – Draft Conclusions Proposed by the President* (United Nations Framework Convention on Climate Change Secretariat, Bonn, Germany, 2005).
14. R. Houghton *et al.*, *Carbon Manage.* **1**, 253–259.
15. H. Geist, E. Lambin, *Bioscience* **52**, 143–150 (2002).
16. S. S. Saatchi *et al.*, *Proc. Natl. Acad. Sci. U.S.A.* **108**, 9899–9904 (2011).
17. A. Baccini *et al.*, *Nature Clim. Change* **2**, 182–185 (2012).
18. N. L. Harris *et al.*, *Science* **336**, 1573–1576 (2012).
19. R. Waterworth, G. Richards, C. Brack, D. Evans, *For. Ecol. Manage.* **238**, 231–243 (2007).
20. P. Potapov *et al.*, *Ecol. Soc.* **13**, 51 (2008).
21. T. M. Brooks *et al.*, *Science* **313**, 58–61 (2006).
22. A. S. Rodrigues *et al.*, *Nature* **428**, 640–643 (2004).
23. T. Rudel, *Rural Sociol.* **63**, 533–552 (1998).

Acknowledgments: Support for Landsat data analysis and characterization was provided by the Gordon and Betty Moore Foundation, the United States Geological Survey, and Google, Inc. GLAS data analysis was supported by the David and Lucile Packard Foundation. Development of all methods was supported by NASA through its Land Cover and Land Use Change, Terrestrial Ecology, Applied Sciences, and MEaSUREs programs (grants NNH05ZDA001N, NNH07ZDA001N, NNX12AB43G, NNX12AC78G, NNX08AP33A, and NNG06GD95G) and by the U.S. Agency for International Development through its CARPE program. Any use of trade, firm, or product names is for descriptive purposes only and does not imply endorsement by the U.S. government. Results are depicted and viewable online at full resolution: http://earthenginepartners.appspot.com/science-2013-global-forest.

Supplementary Materials

www.sciencemag.org/content/342/6160/850/suppl/DC1
Materials and Methods
Supplementary Text
Figs. S1 to S8
Tables S1 to S5
References (*24*–*40*)

14 August 2013; accepted 15 October 2013
10.1126/science.1244693

Changes in Cytoplasmic Volume Are Sufficient to Drive Spindle Scaling

James Hazel,[1] Kaspars Krutkramelis,[2] Paul Mooney,[1] Miroslav Tomschik,[1] Ken Gerow,[3] John Oakey,[2] J. C. Gatlin[1]*

The mitotic spindle must function in cell types that vary greatly in size, and its dimensions scale with the rapid, reductive cell divisions that accompany early stages of development. The mechanism responsible for this scaling is unclear, because uncoupling cell size from a developmental or cellular context has proven experimentally challenging. We combined microfluidic technology with *Xenopus* egg extracts to characterize spindle assembly within discrete, geometrically defined volumes of cytoplasm. Reductions in cytoplasmic volume, rather than developmental cues or changes in cell shape, were sufficient to recapitulate spindle scaling observed in *Xenopus* embryos. Thus, mechanisms extrinsic to the spindle, specifically a limiting pool of cytoplasmic component(s), play a major role in determining spindle size.

Organelles and other intracellular structures must scale with cell size in order to function properly. Maintenance of these dimensional relationships is challenged by the rapid and reductive cell divisions that characterize early embryogenesis in many organisms. The cellular machine that drives these divisions, the mitotic spindle, functions to segregate chromosomes in cells that vary greatly in size while also adapting to rapid changes in cell size. The issue of scale is epitomized during *Xenopus* embryogenesis, where a rapid series of divisions reduces cell size 100-fold: from the 1.2-mm-diameter fertilized egg to ~12-μm-diameter cells in the adult frog (*1*). In large blastomeres, spindle length reaches an upper limit that is uncoupled from changes in cell size. However, as cell size decreases, a strong correlation emerges between spindle length and cell size (*2*). Although this scaling relationship has been characterized in vivo for several different organisms, little is known about the direct regulation of spindle size by cell size or the underlying mechanism(s) (*2*–*4*). Spindle size may be directly dictated by the physical dimensions of a cell, perhaps through microtubule-mediated interaction with the cell cortex [i.e., boundary sensing (*5*–*7*)]. Alternatively, cell size could constrain spindle size by providing a fixed and finite cytoplasmic volume and, therefore, a limiting pool of resources such as cytoplasmic spindle assembly or length-determining components [i.e., component limitation (*8*, *9*)]. Last, mechanisms intrinsic to the spindle could be actively tuned in response to systematic changes in cytoplasmic composition occurring during development [i.e., developmental cues (*10*, *11*)].

To elucidate the responsible scaling mechanism(s), we developed a microfluidic-based platform to confine spindle assembly in geometrically defined volumes of *Xenopus* egg extract (*12*). Interphase extract containing *Xenopus* sperm nuclei was induced to enter mitosis and immediately pumped into a microfluidic droplet-generating device before nuclear envelope breakdown and the onset of spindle assembly. At the same time, a fluorinated oil/surfactant mixture was pumped into the device through a second inlet. These two discrete, immiscible phases merged at a T-shaped junction within the device to produce stable emulsions of extract droplets in a continuous oil phase (Fig. 1, A and C). Changing the T-junction channel dimensions and relative flow rates of the two phases

[1]Department of Molecular Biology, University of Wyoming, Laramie, WY 82071, USA. [2]Department of Chemical and Petroleum Engineering, University of Wyoming, Laramie, WY 82071, USA. [3]Department of Statistics, University of Wyoming, Laramie, WY 82071, USA.

*Corresponding author. E-mail: jgatlin@uwyo.edu

www.sciencemag.org/content/342/6160/850/suppl/DC1

Supplementary Materials for

High-Resolution Global Maps of 21st-Century Forest Cover Change

M. C. Hansen,* P. V. Potapov, R. Moore, M. Hancher, S. A. Turubanova, A. Tyukavina, D. Thau, S. V. Stehman, S. J. Goetz, T. R. Loveland, A. Kommareddy, A. Egorov, L. Chini, C. O. Justice, J. R. G. Townshend

*Corresponding author. E-mail: mhansen@umd.edu

Published 15 November 2013, *Science* **342**, 850 (2013)
DOI: 10.1126/science.1244693

This PDF file includes:

Materials and Methods

The study area included all global land except for Antarctica and a number of Arctic islands, totaling 128.8Mkm^2, or the equivalent of 143 billion 30m Landsat pixels. For this study, trees were defined as all vegetation taller than 5m in height. Forest loss was defined as a stand-replacement disturbance. Results were disaggregated by reference percent tree cover stratum (e.g. >50% crown cover to ~0% crown cover) and by year. Forest degradation (*24*), for example selective removals from within forested stands that do not lead to a non-forest state, was not included in the change characterization. Gain was defined as the inverse of loss, or a non-forest to forest change; longer-lived regrowing stands of tree cover that did not begin as non-forest within the study period were not mapped as forest gain. Gain was related to percent tree crown cover densities >50% and reported as a twelve year total. In this study, the term "forest" refers to tree cover and not land use unless explicitly stated, e.g. "forest land use".

The global Landsat analysis was performed using Google Earth Engine, a cloud platform for earth observation data analysis that combines a public data catalog with a large-scale computational facility optimized for parallel processing of geospatial data. Google Earth Engine contains a nearly complete set of imagery from the Landsat 4, 5, 7, and 8 satellites downloaded from the USGS Earth Resources Observation and Science archive (*25*). For this study, we analyzed 654,178 growing season Landsat 7 Enhanced Thematic Mapper Plus (ETM+) scenes from a total of 1.3 million available at the time of the study. Growing season data are more appropriate for land cover mapping than imagery captured during senescence or dormant seasonal periods (*26*). Automated Landsat pre-processing steps included: (i) image resampling, (ii) conversion of raw digital values (DN) to top of atmosphere (TOA) reflectance, (iii) cloud/shadow/water screening and quality assessment (QA), and (iv) image normalization. All pre-processing steps were tested at national scales around the globe using a method prototyped for the Democratic Republic of Congo (*27*). The stack of QA layers was used to create a per-pixel set of cloud-free image observations which in turn was employed to calculate time-series spectral metrics. Metrics represent a generic feature space that facilitates regional-scale mapping and have been used extensively with MODIS and AVHRR data (*2,4*) and more recently with Landsat data in characterizing forest cover loss (*27,28*). Three groups of per-band metrics were employed over the study interval: (i) reflectance values representing maximum, minimum and selected percentile values (10, 25, 50, 75 and 90% percentiles); (ii) mean reflectance values for observations between selected percentiles (for the max-10%, 10-25%, 25-50%, 50-75%, 75-90%, 90%-max, min-max, 10-90%, and 25-75% intervals); and (iii) slope of linear regression of band reflectance value versus image date. Training data to relate to the Landsat metrics were derived from image interpretation methods, including mapping of crown/no crown categories using very high spatial resolution data such as Quickbird imagery, existing percent tree cover layers derived from Landsat data (*29*), and global MODIS percent tree cover (*30*), rescaled using the higher spatial resolution percent tree cover data sets. Image interpretation on-screen was used to delineate change and no change training data for forest cover loss and gain.

Percent tree cover, forest loss and forest gain training data were related to the time-series metrics using a decision tree. Decision trees are hierarchical classifiers that predict class membership by recursively partitioning a data set into more homogeneous or less

varying subsets, referred to as nodes (*31*). For the tree cover and change products, a bagged decision tree methodology was employed. Forest loss was disaggregated to annual time scales using a set of heuristics derived from the maximum annual decline in percent tree cover and the maximum annual decline in minimum growing season Normalized Vegetation Difference Index (NDVI). Trends in annual forest loss were derived using an ordinary least squares slope of the regression of *y*=annual loss versus *x*=year. Outputs per pixel include annual percent tree cover, annual forest loss from 2000 to 2012, and forest gain from 2000 to 2012. To facilitate processing, each continent was characterized individually: North America, South America, Eurasia, Africa, and Australia.

Earth Engine uses a lazy computation model in which a sequence of operations may be executed either interactively on-the-fly or in bulk over a complete data set. We used the former mode during development and debugging, and the latter mode during the computation of the final data products. In both cases all image processing operations were performed in parallel across a large number of computers, and the platform automatically handled data management tasks such as data format conversion, reprojection and resampling, and associating image metadata with pixel data. Large-scale computations were managed using the FlumeJava framework (*32*). A total of 20 terapixels of data were processed using one million CPU-core hours on 10,000 computers in order to characterize year 2000 percent tree cover and subsequent tree cover loss and gain through 2012.

Supplementary Text

Comparison with FAO data

The standard reference for global scale forest resource information is the UNFAO's Forest Resource Assessment (FRA) (*33*), produced at decadal intervals. There are several limitations of the FRA reports that diminish their utility for global change assessments, including (i) inconsistent methods between countries; (ii) defining "forest" based on land use instead of land cover thereby obscuring the biophysical reality of whether tree cover is present; (iii) forest area changes reported only as net values; and (iv) forest definitions used in successive reports have changed over time (*34*).

Several discrepancies exist between FAO and earth observation-derived forest area change data. For example, the large amount of tree cover change observed in satellite imagery in Canada and the USA does not conform to the land use definitions applied in the FRA for these countries. While there is significant forest change from a biophysical perspective (i.e., forest cover), there is little or no land use change, the main criterion used in the FRA report. Additionally, China, and to a lesser extent India, report significant forest gains that are not readily observable in time-series satellite imagery, including this analysis (Fig. S3). Large country change area discrepancies such as these preclude a significant correlation between FAO and Landsat-based country data at the global scale. However, regional differences in strength of agreement exist, and examples are illustrated in Fig. S3 and Tab. S4. The region with the highest correlation between FAO and Landsat net change is Latin America. Deforestation is the dominant dynamic, and a number of countries, including Brazil, employ earth observation data in estimating forest area change for official reporting. There is much less agreement for African countries, though the correlation improves when lowering the tree cover threshold to

include more change. The lack of agreement in Africa reflects the difficult nature of mapping change in environments with a range of tree cover as well as the lack of systematic forest inventories and mapping capabilities for many African countries. Southeast Asian countries exhibit changes primarily in dense canopy forests. However, there is little correlation between Landsat-based change estimates and FAO data. The forestry dynamics and differing governance and development contexts within this region may lead to inconsistencies between countries. European data have the least correlation of the regions examined, with comparatively little net area change reported in either our Landsat analysis or in the FAO FRA.

The importance of forest definition and its impact on change area estimation is seen for countries located in boreal and dry tropical climates. Our estimate of Canada's net change from the Landsat-based study doubled when including forest loss across all tree cover strata, largely due to extensive burning in open boreal woodlands. Countries such as Australia, Paraguay and Mozambique have similar outcomes related to disturbances occurring within a range of tropical forest, woodland and parkland environments.

Gross forest area gain and loss for >50% tree cover were also compared to FAO roundwood production data summed by country from 2000 to 2011 (Fig. S4). FAO data are available at http://faostat.fao.org/. The national coniferous and non-coniferous "total roundwood" production data (in cubic meters) were multiplied by 0.225MgC/m^3 and 0.325 MgC/m^2 respectively, and then added together to give national total roundwood production in Megatons of carbon. Tab. S4 illustrates the strength of the relationship between FRA roundwood production and Landsat-derived gross forest area gain and loss for selected regions. While Africa and Southeast Asia have extremely poor correlations, Landsat-derived forest area gain for Latin America and both forest gain and loss for Europe exhibit strong correlations. The FRA roundwood production data correlate well with satellite-based tree cover change area estimation for forestry land use-dominated countries.

The FAO comparison reflects the confusion that results when comparing tabular data that apply differing criteria in defining forest change. Deforestation is the conversion of natural forests to non-forest land uses; the clearing of the same natural forests followed by natural recovery or managed forestry is not deforestation and often goes undocumented, whether in the tropical or boreal domains. Understanding where such changes occur is impossible given the current state of knowledge, i.e. the FAO FRA. While countries such as Canada and Indonesia both clear natural forests without conversion to non-forest land uses, Indonesia reports over 5,000km^2 per year of forest area loss in the FRA while Canada reports no change. Consistent, transparent and spatio-temporally explicit quantification of natural and managed forest change is required to fully understand forest change from a biophysical and not solely forest land use perspective.

Recent global forest mapping research

The FAO and others have turned to earth observation data, specifically Landsat imagery, to provide a more consistent depiction of global forest change. Sample-based methods have enabled national to global scale estimation of forest extent and change (*35*,*2*,*3*). Such methods result in tabular aggregated estimates for areas having sufficient sampling densities, but do not allow for local-scale area estimation or spatially explicit representation of extent and change. While exhaustive land cover mapping using Landsat

data has been prototyped using single best-date image methods (*36,37*) based on the National Aeronautics and Space Administration (NASA)-United States Geological Survey (USGS) Global Land Survey data set (*38*), data mining of the Landsat archive to quantify global forest cover change has not been implemented until this study.

Validation

The validation exercise was performed independently of the mapping exercise. Areas of forest loss and gain were validated using a probability-based stratified random sample of 120m blocks per biome. Boreal forest, temperate forest, humid tropical forest and dry tropical forest biomes and other land constituted the five major strata, and were taken from our previous study on global forest cover loss (*2*). The map product was used to create three sub-strata per biome: no change, loss and gain. The sample allocation for each biome was 150 blocks for no change, 90 for change and 60 for gain (1,500 blocks total). Each 120m sample block was interpreted into quartiles of reference change as gain or loss (i.e., the proportion of gain or loss was interpreted as 0, 0.25, 0.50, 0.75, or 1), where reference change was obtained as follows. Image interpretation of time-series Landsat, MODIS and very high spatial imagery from GoogleEarth, where available, was performed in estimating reference change for each sample block. Forest loss estimated from the validation reference data set totaled 2.2Mkm^2 (SE of 0.3Mkm^2) compared to the map total of 2.3Mkm^2. Forest gain estimated from the validation sample totaled 0.9Mkm^2 (SE of 0.2 Mkm^2) compared to the map total of 0.8Mkm^2. Fig. S5 shows the results as mean map and validation change per block for the globe and per FAO climate domain. Fig. S6 illustrates the mean per block difference of the map and reference loss and gain estimates. Comparable map and reference loss and gain results were achieved at the global and climate domain scales.

Estimated error matrices and accuracy summary statistics are shown in Tab. S5. For loss, user's and producer's accuracies are balanced and greater than 80% per climate domain and the globe as a whole. Results for forest gain indicate a possible underestimate of tropical forest gain with a user's accuracy of 82% and a producer's accuracy of 48%. However, the 95% confidence interval for the bias of tropical forest gain (expressed as a % of land area) is 0.01% to 0.35%, indicating high uncertainty in the validation estimate. A possible overestimate of boreal forest gain is also indicated. Overall, the comparison of individually interpreted sample sites with the algorithm output illustrates a robust product at the 120m pixel scale.

The annual allocation of change was validated using annual growing season NDVI imagery from the MODIS sensor. All validation sample blocks were interpreted and if a single, unambiguous drop in NDVI was observed in the MODIS NDVI time series, a year of disturbance was assigned. Only 56% of the validation sample blocks were thus assigned. The sample blocks interpreted represented 46% of the total forest loss mapped with the Landsat imagery, a fraction similar to the 50% ratio of MODIS to Landsat-detected change in a previous global forest cover loss study (*39*). For the interpreted blocks, the mean deviation of the loss date was 0.06 years and the mean absolute deviation was 0.29 years. The year of disturbance matched for 75.2% of the forest loss events and 96.7% of the loss events occurred within one year before or after the estimated year of disturbance.

A second evaluation of forest change was made using LiDAR (light detection and ranging) data from NASA's GLAS (Geoscience Laser Altimetry System) instrument onboard the IceSat-1 satellite. Global GLAS release 28 (L1A Global Altimetry Data and

the L2 Global Land Surface Altimetry Data) data were screened for quality and viable GLAS shots used to calculate canopy height (*40*). For forest loss, GLAS shots co-located with Landsat forest loss by pixel were identified. The Landsat-estimated year of disturbance was subtracted from the year of the GLAS shots and populations of 'year since disturbance' created. Significant differences in height before and after Landsat-derived forest loss indicate both a reasonable approximation of forest loss and year of disturbance. Fig. S7 shows the results by ecozone, all of which passed Wilcoxon-Mann-Whitney significance tests (non-parametric alternative of t-test) for pairs of +1\-1 and +2\-2 years.

Forest gain was not allocated annually, but over the entire study period. To compare GLAS-derived change in height with Landsat-derived gain, gain-identified pixels with no tree cover for year 2000 and co-located with GLAS data were analyzed. Additionally, only clustered gain was analyzed, specifically sites where six out of nine pixels within a 3x3 kernel were labeled as forest gain. Fig. S8 illustrates the results. All climate domains except for the boreal passed Wilcoxon-Mann-Whitney significance tests for 2004 and 2008, the beginning and end years for GLAS data collection. The growth-limiting climate of the boreal domain would preclude the observation of regrowth over such a short period.

Table S1. Climate domain tree cover extent, loss and gain summary statistics (km^2), ranked by total loss.

.

Climate Domain	Total Loss	Total Gain	Treecover 2000				Loss within treecover				Total loss / total land area (excluding water) (%)	>25% tree cover loss / year 2000 >25% tree cover (%)	>50% tree cover loss / year 2000 >50% tree cover (%)	>75% tree cover loss / year 2000 >75% tree cover (%)	Total gain / year 2000 >50% tree cover (%)	>50% loss + total gain / 2000 >50% tree cover (%)	Previous column less double counting pixels with both loss and gain (%)
			<25%	26-50%	51-75%	76-100%	<25%	26-50%	51-75%	76-100%							
a)	b)	c)	d)	e)	f)	g)	h)	i)	j)	k)	l)	m)	n)	o)	p)	q)	r)
Tropical	1105786	247233	35866276	4175597	3524230	13241470	85479	125921	180106	714278	1.9	4.9	5.3	5.4	1.5	6.8	6.3
Boreal	606841	207100	11066215	2988449	3782283	4360312	51285	114990	147631	292935	2.7	5.0	5.4	6.7	2.5	8.0	7.9
Subtropical	305835	194103	19087918	769954	829023	1830148	37924	28761	32363	206787	1.4	7.8	9.0	11.3	7.3	16.3	13.8
Temperate	273390	155989	20938580	676500	1195036	4080868	7856	11588	25881	228064	1.0	4.5	4.8	5.6	3.0	7.8	7.5
Total	2291851	804425	86958989	8610500	9330573	23512797	182544	281261	385982	1442065	1.8	5.1	5.6	6.1	2.4	8.0	7.5

Table S2. Ecozone tree cover extent, loss and gain summary statistics (km^2), ranked by total loss.

Ecozones by vegetation realm AFR – Africa AUS – Australia/Oceania EAS –Eurasia NAM – North America SAM – South America a)	Total Loss b)	Total Gain c)	Treecover 2000				Loss within treecover				Total loss / total land area (excluding water) (%) l)	>25% tree cover loss / year 2000 >25% tree cover (%) m)	>50% tree cover loss / year 2000 >50% tree cover (%) n)	>75% tree cover loss / year 2000 >75% tree cover (%) o)	Total gain / year 2000 >50% tree cover (%) p)	>50% loss + total gain / 2000 >50% tree cover (%) q)	Previous column less double counting pixels with both loss and gain (%) r)
			<25% d)	26-50% e)	51-75% f)	76-100% g)	<25% h)	26-50% i)	51-75% j)	76-100% k)							
SAM Tropical rainforest	253435	33042	678685	100431	131817	5607324	2125	3847	10919	236544	3.9	4.3	4.3	4.2	0.6	4.9	4.7
EAS Boreal coniferous forest	229331	124488	1774827	904244	1577094	1831760	15280	29602	50285	134164	3.8	5.0	5.4	7.3	3.7	9.1	9.0
EAS Tropical rainforest	228011	104488	563048	116976	275092	1661696	2666	2856	15050	207438	8.7	11.0	11.5	12.5	5.4	16.9	14.4
SAM Tropical moist deciduous forest	162095	33615	2456904	379932	404571	1003315	17675	25214	36530	82676	3.8	8.1	8.5	8.2	2.4	10.9	10.2
EAS Boreal mountain system	143573	36555	2266444	756678	1000381	1048086	23000	30952	38751	50869	2.8	4.3	4.4	4.9	1.8	6.2	6.1
NAM Subtropical humid forest	122915	103420	399595	55264	65639	522260	854	1582	6486	113993	11.8	19.0	20.5	21.8	17.6	38.1	31.2
NAM Boreal coniferous forest	120804	39978	314668	264683	474734	917683	3223	21444	22386	73751	6.1	7.1	6.9	8.0	2.9	9.8	9.5
AFR Tropical rainforest	96848	24575	511549	752270	742393	1941290	2272	10590	28693	55293	2.5	2.8	3.1	2.8	0.9	4.0	3.7
SAM Tropical dry forest	88784	3032	898296	382134	231661	150647	10581	30683	29104	18416	5.3	10.2	12.4	12.2	0.8	13.2	13.1
AFR Tropical moist deciduous forest	84719	3649	2370104	1331743	845218	40070	27852	28032	25474	3361	1.8	2.6	3.3	8.4	0.4	3.7	3.5
NAM Temperate mountain system	82998	39105	791649	107937	153970	891664	2385	4274	6475	69864	4.3	7.0	7.3	7.8	3.7	11.0	10.7
NAM Boreal tundra woodland	63370	4342	924788	659389	405281	284991	3266	21744	20580	17779	2.8	4.5	5.6	6.2	0.6	6.2	6.2
EAS Temperate continental forest	63068	48939	3126680	210065	500447	1003265	1118	2023	9041	50886	1.3	3.6	4.0	5.1	3.3	7.2	7.1
NAM Temperate continental forest	56749	26139	731687	80291	131018	1000282	216	549	2045	53939	2.9	4.7	4.9	5.4	2.3	7.3	6.9
EAS Subtropical humid forest	44693	17066	989723	193841	339619	469305	1208	1962	10323	31200	2.2	4.3	5.1	6.6	2.1	7.2	6.6
NAM Boreal mountain system	39485	1332	568948	180517	189178	233314	1145	8887	13879	15573	3.4	6.4	7.0	6.7	0.3	7.3	7.3
AFR Tropical dry forest	33259	3298	3076095	412938	125125	19520	11240	11866	7820	2332	0.9	3.9	7.0	11.9	2.3	9.3	8.2
EAS Tropical moist deciduous forest	28166	7837	739252	91874	189904	298608	1829	1938	6724	17674	2.1	4.5	5.0	5.9	1.6	6.6	6.2
NAM Tropical moist deciduous forest	25169	8174	284373	55814	73719	247384	737	1413	3932	19087	3.8	6.5	7.2	7.7	2.5	9.7	9.4
NAM Tropical rainforest	22777	2641	97950	23299	36653	253265	202	470	1770	20334	5.5	7.2	7.6	8.0	0.9	8.5	8.4
EAS Temperate oceanic forest	19089	13471	929909	40517	84314	216456	379	640	2583	15488	1.5	5.5	6.0	7.2	4.5	10.5	10.0
EAS Temperate mountain system	19037	8892	4100378	101904	174080	568263	995	1449	2534	14058	0.4	2.1	2.2	2.5	1.2	3.4	3.4
NAM Subtropical mountain system	18861	5631	370255	56439	45414	117601	2137	2207	2500	12018	3.2	7.6	8.9	10.2	3.5	12.4	11.5
SAM Subtropical humid forest	17149	25269	971549	38429	40670	132183	491	648	1350	14660	1.4	7.9	9.3	11.1	14.6	23.9	20.5
SAM Tropical mountain system	15624	4700	1154706	64730	90321	559185	561	799	1303	12961	0.8	2.1	2.2	2.3	0.7	2.9	2.7
EAS Tropical mountain system	14459	5388	301136	34772	93240	350957	304	495	2473	11189	1.9	3.0	3.1	3.2	1.2	4.3	3.9
EAS Tropical dry forest	13952	1755	1181479	74787	75701	67938	1575	1586	3699	7093	1.0	5.7	7.5	10.4	1.2	8.7	8.5
AFR Tropical mountain system	12236	4813	1098346	176193	80558	107352	1040	2161	3400	5635	0.8	3.1	4.8	5.2	2.6	7.4	6.8
EAS Subtropical dry forest	10987	5120	734840	62992	48342	87437	1515	1729	2677	5066	1.2	4.8	5.7	5.8	3.8	9.5	8.7

AUS Tropical rainforest	9972	3374	48615	20176	30783	687847	65	97	345	9465	1.3	1.3	1.4	1.4	0.5	1.8	1.7
EAS Subtropical mountain system	9695	4213	3012481	116266	177782	285763	726	1155	2571	5243	0.3	1.5	1.7	1.8	0.9	2.6	2.5
EAS Boreal tundra woodland	8300	286	1081882	150336	86494	15996	4393	1951	1432	524	0.6	1.5	1.9	3.3	0.3	2.2	2.2
SAM Subtropical dry forest	8256	10797	57044	5787	6298	30265	49	84	269	7854	8.3	19.4	22.2	26.0	29.5	51.7	42.5
AUS Subtropical humid forest	6488	5983	130692	22580	30269	90635	82	206	394	5806	2.4	4.5	5.1	6.4	4.9	10.1	8.5
AUS Temperate oceanic forest	5439	5786	108801	6052	13996	82774	24	54	216	5146	2.6	5.3	5.5	6.2	6.0	11.5	9.6
AFR Subtropical mountain system	5180	5137	390362	9522	6115	5316	295	536	1898	2451	1.3	23.3	38.0	46.1	44.9	83.0	58.1
AUS Subtropical dry forest	4234	3902	81757	17375	10024	12111	417	1037	886	1894	3.5	9.7	12.6	15.6	17.6	30.2	25.4
AUS Temperate mountain system	4220	2269	94608	14214	21282	60561	35	68	257	3860	2.2	4.4	5.0	6.4	2.8	7.8	6.8
SAM Temperate oceanic forest	3292	3510	107543	8332	23900	90484	41	15	45	3192	1.4	2.6	2.8	3.5	3.1	5.9	4.9
NAM Tropical dry forest	3177	870	142817	31827	25026	22140	283	616	1151	1127	1.4	3.7	4.8	5.1	1.8	6.7	6.6
NAM Temperate oceanic forest	2854	2317	14521	1511	1900	20962	7	12	35	2801	7.3	11.7	12.4	13.4	10.1	22.5	20.1
NAM Tropical mountain system	2832	522	123244	30126	31947	72471	113	236	448	2035	1.1	2.0	2.4	2.8	0.5	2.9	2.8
AFR Subtropical dry forest	1864	880	308429	10588	7605	8179	224	341	526	772	0.6	6.2	8.2	9.4	5.6	13.8	12.9
NAM Subtropical dry forest	1717	723	67075	3801	3009	12153	128	170	238	1181	2.0	8.4	9.4	9.7	4.8	14.1	13.0
AFR Subtropical humid forest	1556	1229	58127	14101	8704	3540	74	160	517	805	1.8	5.6	10.8	22.7	10.0	20.8	15.0
AUS Tropical mountain system	751	317	7778	3977	7622	101354	4	9	46	691	0.6	0.7	0.7	0.7	0.3	1.0	0.9
AUS Tropical dry forest	707	379	414034	31011	7067	8741	312	222	82	91	0.2	0.8	1.1	1.0	2.4	3.5	2.1
AUS Tropical moist deciduous forest	375	94	10919	7706	10154	25954	4	7	46	317	0.7	0.8	1.0	1.2	0.3	1.3	1.2
SAM Temperate mountain system	248	142	52497	1603	3662	17420	15	3	8	221	0.3	1.0	1.1	1.3	0.7	1.8	1.7
SAM Subtropical mountain system	147	119	226487	2143	1706	7185	8	3	7	129	0.1	1.3	1.5	1.8	1.3	2.9	2.6

Table S3. Country tree cover extent, loss and gain summary statistics (km^2), ranked by total loss.

Country	Total loss	Total gain	Treecover 2000				Loss within treecover				Total loss / total land area (excluding water) (%)	>25% tree cover loss / year 2000 >25% tree cover (%)	>50% tree cover loss / year 2000 >50% tree cover (%)	>75% tree cover loss / year 2000 >75% tree cover (%)	Total gain / year 2000 >50% tree cover (%)	>50% loss + total gain / 2000 >50% tree cover (%)	Previous column less double counting pixels with both loss and gain (%)
			<25%	26-50%	51-75%	76-100%	<25%	26-50%	51-75%	76-100%							
a)	b)	c)	d)	e)	f)	g)	h)	i)	j)	k)	l)	m)	n)	o)	p)	q)	r)
Russia	365015	162292	8414687	1846554	2707260	3304608	43907	62789	88346	169972	2.2	4.1	4.3	5.1	2.7	7.0	7.0
Brazil	360277	75866	3118579	509317	464530	4292417	23699	30816	43577	262185	4.3	6.4	6.4	6.1	1.6	8.0	7.5
United States	263944	138082	6294153	424662	462709	1982786	9274	17956	30306	206408	2.9	8.9	9.7	10.4	5.6	15.3	13.4
Canada	263943	91071	4141357	1068282	1074635	2167262	6860	44780	46295	166007	3.1	6.0	6.5	7.7	2.8	9.4	9.1
Indonesia	157850	69701	252964	68334	141996	1411892	1558	1611	8887	145795	8.4	9.6	10.0	10.3	4.5	14.4	12.4
China	61130	22387	7565646	387994	694764	618901	2250	3955	17457	37469	0.7	3.5	4.2	6.1	1.7	5.9	5.5
DRCongo	58963	13926	175163	469228	453121	1190506	917	4863	12362	40821	2.6	2.7	3.2	3.4	0.8	4.1	3.8
Australia	58736	14142	7209820	209287	79484	177890	28168	17318	2335	10915	0.8	6.6	5.1	6.1	5.5	10.6	9.1
Malaysia	47278	25798	32061	5538	17263	272365	289	309	1818	44862	14.4	15.9	16.1	16.5	8.9	25.0	20.6
Argentina	46958	6430	2352414	170266	125227	105950	5039	14574	14378	12966	1.7	10.4	11.8	12.2	2.8	14.6	13.9
Paraguay	37958	510	146165	110139	64482	75473	1230	12592	11751	12385	9.6	14.7	17.2	16.4	0.4	17.6	17.6
Bolivia	29867	1736	424460	75142	96512	478387	464	1340	4295	23768	2.8	4.5	4.9	5.0	0.3	5.2	5.1
Sweden	25533	15281	130774	42494	85855	153996	95	302	1790	23346	6.2	9.0	10.5	15.2	6.4	16.9	16.6
Colombia	25193	5516	302224	41544	61240	721695	315	619	1943	22315	2.2	3.0	3.1	3.1	0.7	3.8	3.7
Mexico	23862	6333	1391412	131003	126317	294988	1919	2013	4042	15887	1.2	4.0	4.7	5.4	1.5	6.2	6.0
Mozambique	21552	1446	403453	266480	101514	3414	3078	10181	7818	476	2.8	5.0	7.9	13.9	1.4	9.3	8.8
Tanzania	19903	3041	544450	243832	84708	12320	5111	7880	5740	1173	2.2	4.3	7.1	9.5	3.1	10.3	9.5
Finland	19516	10849	85929	36353	78775	104264	74	263	1684	17496	6.4	8.9	10.5	16.8	5.9	16.4	16.3
Angola	19320	638	612241	314210	281472	37883	4423	6556	6579	1762	1.6	2.4	2.6	4.7	0.2	2.8	2.8
Peru	15288	1910	498646	14200	23555	744591	80	101	245	14863	1.2	1.9	2.0	2.0	0.2	2.2	2.1
Myanmar	14958	3149	227580	37863	123465	274434	556	896	3991	9514	2.3	3.3	3.4	3.5	0.8	4.2	3.9
Cote d'Ivoire	14889	2298	139172	116351	58468	5111	2893	3830	6953	1213	4.7	6.7	12.8	23.7	3.6	16.5	15.5
Madagascar	14659	4051	402077	64144	63773	58637	1382	2490	4900	5888	2.5	7.1	8.8	10.0	3.3	12.1	10.8
Zambia	13163	181	419962	224188	91539	429	3460	5562	3918	223	1.8	3.1	4.5	52.0	0.2	4.7	4.7
Venezuela	12958	1910	328461	33724	43779	493663	695	993	2389	8881	1.4	2.1	2.1	1.8	0.4	2.5	2.4
Cambodia	12595	1096	86064	16785	16401	58431	484	748	2478	8884	7.1	13.2	15.2	15.2	1.5	16.6	16.1
Vietnam	12289	5643	152816	22284	40869	106971	660	637	2247	8744	3.8	6.8	7.4	8.2	3.8	11.3	10.5
Laos	12084	3379	34908	11904	36244	144908	384	422	1861	9417	5.3	6.1	6.2	6.5	1.9	8.1	7.2
Thailand	12049	4992	301598	25899	69216	110454	1402	1050	2985	6612	2.4	5.2	5.3	6.0	2.8	8.1	7.7
Chile	11879	14611	546019	17728	36107	142031	112	107	331	11329	1.6	6.0	6.5	8.0	8.2	14.7	12.2

Nigeria	10239	603	772371	82016	44023	3125	5987	2670	1435	147	1.1	3.3	3.4	4.7	1.3	4.6	4.4
South Africa	9526	8313	1145626	39602	20818	10826	678	1074	3365	4411	0.8	12.4	24.6	40.7	26.3	50.8	36.2
India	8971	2549	2703530	112692	136677	167827	810	855	2117	5189	0.3	2.0	2.4	3.1	0.8	3.2	3.0
Guatemala	8883	1094	29734	8709	11952	57571	105	323	1097	7357	8.2	11.2	12.2	12.8	1.6	13.7	13.4
Nicaragua	8225	662	39402	8527	12384	58289	109	230	650	7236	6.9	10.2	11.2	12.4	0.9	12.1	12.0
France	7664	5062	373705	19842	37021	115684	209	330	1149	5977	1.4	4.3	4.7	5.2	3.3	8.0	7.6
Spain	6908	4482	386553	36472	28533	52468	676	982	1698	3552	1.4	5.3	6.5	6.8	5.5	12.0	11.4
New Zealand	6883	7102	149606	5653	14375	93838	24	22	126	6711	2.6	6.0	6.3	7.2	6.6	12.9	10.7
Papua New Guinea	6337	2308	27933	11647	23295	396660	29	35	197	6076	1.4	1.5	1.5	1.5	0.5	2.0	1.9
Philippines	6227	2726	102570	15788	33051	141108	84	90	485	5569	2.1	3.2	3.5	3.9	1.6	5.0	4.7
Poland	5829	5041	201808	11013	30655	64857	79	163	814	4773	1.9	5.4	5.8	7.4	5.3	11.1	10.7
Ukraine	5657	3529	470946	19510	28312	68474	150	234	900	4372	1.0	4.7	5.4	6.4	3.6	9.1	8.8
Ghana	5406	1345	153157	36659	40464	2074	911	1099	2863	533	2.3	5.7	8.0	25.7	3.2	11.1	10.3
Ecuador	5246	1027	62024	12832	20737	158764	58	118	373	4697	2.1	2.7	2.8	3.0	0.6	3.4	3.3
Portugal	4987	2866	64476	8726	6753	9147	459	784	1246	2497	5.6	18.4	23.5	27.3	18.0	41.6	36.1
Germany	4890	2585	226231	10219	25175	91960	61	79	457	4294	1.4	3.8	4.1	4.7	2.2	6.3	6.1
Honduras	4860	582	32713	11870	14297	52664	84	238	560	3978	4.4	6.1	6.8	7.6	0.9	7.6	7.6
Cameroon	4816	651	120385	90110	77877	174702	548	691	1595	1981	1.0	1.2	1.4	1.1	0.3	1.7	1.6
Mongolia	4779	103	1508028	26031	15552	3080	857	1514	1485	922	0.3	8.8	12.9	29.9	0.6	13.5	13.5
Central African Republic	4719	395	101812	209547	238922	68765	226	910	1869	1714	0.8	0.9	1.2	2.5	0.1	1.3	1.3
Japan	4303	2570	102902	9616	22119	233863	71	57	253	3924	1.2	1.6	1.6	1.7	1.0	2.6	2.5
Belarus	4167	3755	112240	8835	25820	57913	26	89	547	3504	2.0	4.5	4.8	6.1	4.5	9.3	9.1
Latvia	4120	1857	27713	2742	7086	26126	10	32	253	3825	6.5	11.4	12.3	14.6	5.6	17.9	17.6
Liberia	3955	1084	1221	3783	54435	36117	7	96	2305	1547	4.1	4.2	4.3	4.3	1.2	5.5	4.9
Guinea	3933	296	130230	91912	19736	1821	1251	1604	923	155	1.6	2.4	5.0	8.5	1.4	6.4	6.1
Zimbabwe	3869	486	362829	21175	2132	799	2284	1018	353	214	1.0	6.6	19.3	26.8	16.6	35.9	29.2
Uganda	3654	685	105539	67065	24230	8489	154	703	1118	1679	1.8	3.5	8.5	19.8	2.1	10.6	10.2
Norway	3520	1729	187652	21453	35282	62297	18	37	214	3252	1.1	2.9	3.6	5.2	1.8	5.3	5.3
Turkey	3426	1783	664081	24543	23040	59104	535	488	706	1697	0.4	2.7	2.9	2.9	2.2	5.1	4.7
Benin	3307	69	108992	5962	81	8	2835	405	59	8	2.9	7.8	75.3	100.0	77.5	152.8	143.8
Chad	3306	1	1257866	9549	72	0	2914	382	10	0	0.3	4.1	13.9	-	1.4	15.3	15.3
Kenya	3059	1005	530692	20815	9271	9636	732	587	612	1129	0.5	5.9	9.2	11.7	5.3	14.5	13.8
Republic of Congo	2993	467	52860	46265	25236	214202	101	272	803	1819	0.9	1.0	1.1	0.8	0.2	1.3	1.2
Ethiopia	2821	625	968731	100537	33866	20399	375	947	828	671	0.3	1.6	2.8	3.3	1.2	3.9	3.8
United Kingdom	2689	2111	203651	8793	14394	15185	84	167	478	1960	1.1	6.8	8.2	12.9	7.1	15.4	14.9
Panama	2675	323	16563	3089	4854	49687	35	69	262	2308	3.6	4.6	4.7	4.6	0.6	5.3	5.2
Romania	2307	1530	154828	7088	10939	62836	20	25	103	2158	1.0	2.8	3.1	3.4	2.1	5.1	5.0
Estonia	2179	894	16601	2052	5085	19569	5	11	126	2036	5.0	8.1	8.8	10.4	3.6	12.4	12.3
Uruguay	2027	4985	157077	3568	5359	8522	26	73	282	1646	1.2	11.5	13.9	19.3	35.9	49.8	45.2
Austria	2015	658	39299	2743	7205	33933	11	22	130	1853	2.4	4.6	4.8	5.5	1.6	6.4	6.3
Burkina Faso	1993	0	274158	11	0	0	1987	5	0	0	0.7	45.5	-	-	-	-	-
Sierra Leone	1967	451	11320	24844	33463	2424	24	240	1231	472	2.7	3.2	4.7	19.5	1.3	6.0	5.6
Dominican Republic	1929	393	21365	4064	4619	17744	72	120	276	1462	4.0	7.0	7.8	8.2	1.8	9.5	9.4

Gabon	1891	391	11898	8112	10885	230775	27	110	285	1469	0.7	0.7	0.7	0.6	0.2	0.9	0.8
Lithuania	1845	1226	40296	1889	5303	16472	9	20	160	1655	2.9	7.8	8.3	10.0	5.6	14.0	13.7
Cuba	1725	2271	68008	4982	7388	28775	90	126	295	1214	1.6	4.0	4.2	4.2	6.3	10.5	10.4
Mali	1694	0	1247103	1007	3	0	1650	40	3	0	0.1	4.3	100.0	-	0.0	100.0	100.0
Costa Rica	1653	382	11327	2752	5663	31183	28	68	200	1356	3.2	4.1	4.2	4.3	1.0	5.3	5.1
Czech Republic	1646	1331	46934	2445	6429	22264	14	25	197	1410	2.1	5.2	5.6	6.3	4.6	10.2	10.0
South Sudan	1635	38	460581	128358	39278	1773	567	629	356	83	0.3	0.6	1.1	4.7	0.1	1.2	1.1
North Korea	1605	137	67695	12808	31773	9164	96	262	837	411	1.3	2.8	3.0	4.5	0.3	3.4	3.4
Italy	1603	898	201331	13199	19020	64805	113	105	244	1142	0.5	1.5	1.7	1.8	1.1	2.7	2.5
Greece	1566	356	91341	10219	8443	21132	188	181	311	886	1.2	3.5	4.0	4.2	1.2	5.3	5.1
South Korea	1463	271	43787	9776	28496	16694	230	215	560	458	1.5	2.2	2.3	2.7	0.6	2.9	2.8
Malawi	1290	103	71949	19030	2967	163	399	540	309	43	1.4	4.0	11.2	26.4	3.3	14.5	13.8
Slovakia	1237	523	24608	1245	2814	20170	6	11	67	1153	2.5	5.1	5.3	5.7	2.3	7.6	7.4
Belize	1206	128	4073	437	675	16434	5	10	35	1155	5.6	6.8	7.0	7.0	0.7	7.7	7.5
Hungary	1107	1350	71070	2658	3705	14263	12	19	84	992	1.2	5.3	6.0	7.0	7.5	13.5	13.0
Sri Lanka	985	264	24684	4952	9285	26177	64	77	294	551	1.5	2.3	2.4	2.1	0.7	3.1	3.0
Guyana	915	114	18733	1096	1319	187681	4	6	14	890	0.4	0.5	0.5	0.5	0.1	0.5	0.5
Senegal	832	2	192538	1723	20	1	806	23	3	0	0.4	1.5	14.3	0.0	9.5	23.8	23.8
Kazakhstan	828	239	2628744	13973	13954	17598	329	196	125	178	0.0	1.1	1.0	1.0	0.8	1.7	1.7
Bulgaria	779	678	68662	3910	6653	32070	18	20	71	670	0.7	1.8	1.9	2.1	1.8	3.7	3.4
Ireland	778	1238	60220	2358	3492	2899	26	38	122	592	1.1	8.6	11.2	20.4	19.4	30.5	29.0
Togo	768	24	48707	6809	1270	5	383	333	50	2	1.4	4.8	4.1	40.0	1.9	6.0	5.8
Swaziland	747	603	11310	3962	1386	597	48	84	204	412	4.3	11.8	31.1	69.0	30.4	61.5	41.9
Algeria	743	325	2294657	4212	3989	4967	67	136	211	329	0.0	5.1	6.0	6.6	3.6	9.7	9.5
Suriname	724	70	4791	420	567	138564	2	4	9	708	0.5	0.5	0.5	0.5	0.1	0.6	0.5
Guinea-Bissau	676	65	18081	11875	3106	35	164	315	186	11	2.0	3.4	6.3	31.4	2.1	8.3	7.9
Solomon Islands	630	203	528	122	441	26825	3	1	5	621	2.3	2.3	2.3	2.3	0.7	3.0	2.8
Belgium	601	373	21609	1139	2011	5756	7	11	59	524	2.0	6.7	7.5	9.1	4.8	12.3	11.9
El Salvador	567	86	9961	2231	3309	4710	25	56	206	280	2.8	5.3	6.1	5.9	1.1	7.1	7.1
Bangladesh	543	70	108675	5560	8449	6965	15	23	116	389	0.4	2.5	3.3	5.6	0.5	3.7	3.7
Denmark	533	322	35730	1281	2506	3105	8	13	68	444	1.3	7.6	9.1	14.3	5.7	14.9	14.5
Croatia	454	265	31487	2890	3396	18892	53	35	40	326	0.8	1.6	1.6	1.7	1.2	2.8	2.8
French Guiana	441	42	928	110	216	81317	1	1	4	435	0.5	0.5	0.5	0.5	0.1	0.6	0.6
Equatorial Guinea	439	56	199	251	1864	24513	2	12	76	349	1.6	1.6	1.6	1.4	0.2	1.8	1.7
Nepal	434	134	94352	9930	21761	21318	67	65	106	195	0.3	0.7	0.7	0.9	0.3	1.0	1.0
Jamaica	329	68	3185	479	753	6545	7	9	28	285	3.0	4.1	4.3	4.4	0.9	5.2	5.2
Morocco	315	196	405884	2870	2251	2110	58	65	85	107	0.1	3.6	4.4	5.1	4.5	8.9	8.8
Albania	311	74	21128	1719	1711	3642	20	25	55	212	1.1	4.1	5.0	5.8	1.4	6.4	6.3
Macedonia	296	104	16148	1234	1600	5359	11	11	31	244	1.2	3.5	4.0	4.6	1.5	5.4	5.0
Haiti	286	48	17810	2494	2238	4334	19	42	76	148	1.1	2.9	3.4	3.4	0.7	4.1	4.1
Serbia	267	356	49076	3338	5852	19132	5	4	13	245	0.3	0.9	1.0	1.3	1.4	2.5	2.4
Taiwan	267	61	12174	1158	2368	20098	6	7	27	227	0.7	1.1	1.1	1.1	0.3	1.4	1.4
Switzerland	227	104	24221	1255	3120	11363	3	3	19	201	0.6	1.4	1.5	1.8	0.7	2.2	2.2

Burundi	204	36	16600	6956	1189	222	43	86	65	11	0.8	1.9	5.4	5.0	2.6	7.9	7.7
Bosnia and Herzegovina	198	265	23549	2532	4225	20546	26	15	38	120	0.4	0.6	0.6	0.6	1.1	1.7	1.7
Fiji	194	119	2205	1834	1857	12339	1	2	17	174	1.1	1.2	1.3	1.4	0.8	2.2	2.1
East Timor	185	61	7265	1467	1871	4296	4	5	20	156	1.2	2.4	2.9	3.6	1.0	3.8	3.7
Rwanda	178	71	16805	4966	1171	889	22	65	63	27	0.7	2.2	4.4	3.0	3.4	7.8	7.4
Brunei	171	88	434	68	157	5066	2	1	7	161	3.0	3.2	3.2	3.2	1.7	4.9	4.3
Netherlands	166	71	28258	1503	1896	2866	6	8	32	121	0.5	2.6	3.2	4.2	1.5	4.7	4.7
Slovenia	162	35	6851	612	1304	11166	3	3	16	140	0.8	1.2	1.3	1.3	0.3	1.5	1.5
Trinidad and Tobago	154	16	1188	111	168	3664	2	2	9	140	3.0	3.8	3.9	3.8	0.4	4.3	4.2
Puerto Rico	141	64	3591	397	539	4381	10	7	19	105	1.6	2.5	2.5	2.4	1.3	3.8	3.8
Bhutan	129	22	13772	2471	7040	16652	9	13	35	73	0.3	0.5	0.5	0.4	0.1	0.5	0.5
Namibia	128	0	822966	122	5	1	104	21	3	0	0.0	18.8	50.0	0.0	0.0	50.0	50.0
New Caledonia	125	57	3883	4303	3261	7254	7	24	37	57	0.7	0.8	0.9	0.8	0.5	1.4	1.4
Gambia	111	0	10221	213	0	0	99	11	0	0	1.1	5.2	-	-	-	-	-
Tunisia	103	115	152233	568	712	1074	13	12	20	58	0.1	3.8	4.4	5.4	6.4	10.8	10.6
Pakistan	100	8	861788	4077	3320	3349	9	11	35	46	0.0	0.9	1.2	1.4	0.1	1.3	1.3
Bahamas	95	8	8628	571	575	1995	3	6	10	75	0.8	2.9	3.3	3.8	0.3	3.6	3.6
Syria	91	16	184360	319	366	455	10	10	17	54	0.0	7.1	8.6	11.9	1.9	10.6	10.5
Georgia	90	48	37436	2601	4558	25006	5	3	11	71	0.1	0.3	0.3	0.3	0.2	0.4	0.4
Kosovo	90	56	7064	494	959	2388	3	3	7	76	0.8	2.2	2.5	3.2	1.7	4.2	4.0
Montenegro	77	70	6683	899	1309	4194	5	6	16	51	0.6	1.1	1.2	1.2	1.3	2.5	2.5
Azerbaijan	76	9	71829	2175	2938	8193	9	8	17	43	0.1	0.5	0.5	0.5	0.1	0.6	0.6
Somalia	76	3	631245	1191	146	11	44	22	9	1	0.0	2.4	6.4	9.1	1.9	8.3	8.3
Sudan	69	0	1868187	2471	12	0	55	13	1	0	0.0	0.6	8.3	-	0.0	8.3	8.3
Botswana	56	1	577110	529	13	0	47	9	0	0	0.0	1.7	0.0	-	7.7	7.7	7.7
Iran	44	11	1600192	2553	5459	9996	10	5	13	15	0.0	0.2	0.2	0.2	0.1	0.3	0.3
Luxembourg	44	27	1543	59	149	808	1	1	4	39	1.7	4.3	4.5	4.8	2.8	7.3	7.1
Vanuatu	41	14	227	211	630	10997	0	0	2	38	0.3	0.3	0.3	0.3	0.1	0.5	0.5
Moldova	41	63	29783	625	1033	2099	4	4	7	26	0.1	1.0	1.1	1.2	2.0	3.1	3.0
Kyrgyzstan	35	5	185261	2969	2220	2085	12	4	6	12	0.0	0.3	0.4	0.6	0.1	0.5	0.5
Lebanon	32	18	9695	268	249	191	8	5	8	11	0.3	3.4	4.3	5.8	4.1	8.4	8.2
Reunion	31	31	673	489	573	742	1	3	15	12	1.3	1.7	2.1	1.6	2.4	4.4	4.1
Israel	29	19	21626	149	104	77	9	4	7	9	0.1	6.1	8.8	11.7	10.5	19.3	19.3
Mauritius	25	30	1020	326	216	292	2	5	8	11	1.3	2.9	3.7	3.8	5.9	9.6	9.1
Egypt	24	50	974071	3726	140	6	9	8	6	1	0.0	0.4	4.8	16.7	34.2	39.0	39.0
Cyprus	24	2	8057	572	385	231	8	5	5	7	0.3	1.4	1.9	3.0	0.3	2.3	2.3
Martinique	22	5	351	45	81	629	1	1	2	19	2.0	2.9	3.0	3.0	0.7	3.7	3.5
Armenia	21	13	24882	519	698	2252	2	1	3	15	0.1	0.5	0.6	0.7	0.4	1.1	1.1
Afghanistan	20	3	641182	1064	729	755	2	4	8	6	0.0	0.7	0.9	0.8	0.2	1.1	1.1
Guadeloupe	20	12	673	59	84	818	2	1	3	14	1.2	1.9	1.9	1.7	1.3	3.2	3.1
Uzbekistan	15	5	433865	712	309	205	5	3	4	4	0.0	0.9	1.6	2.0	1.0	2.5	2.5
Comoros	7	4	236	350	369	690	0	1	3	4	0.4	0.6	0.7	0.6	0.4	1.0	1.0
Tajikistan	7	1	140238	507	131	63	4	1	1	1	0.0	0.4	1.0	1.6	0.5	1.5	1.5

Turkmenistan	7	3	466423	69	33	25	2	2	1	2	0.0	3.9	5.2	8.0	5.2	10.3	10.3
Libya	7	4	1615869	55	16	3	5	1	0	0	0.0	1.4	0.0	0.0	21.1	21.1	21.1
Cape Verde	4	20	3862	41	13	24	3	0	0	1	0.1	1.3	2.7	4.2	54.1	56.8	56.8
Iraq	3	3	442709	133	58	8	2	0	0	0	0.0	0.0	0.0	0.0	4.5	4.5	4.5
Hong Kong	2	3	436	117	242	280	0	0	1	1	0.2	0.3	0.4	0.4	0.6	1.0	1.0
Lesotho	2	2	30302	110	5	0	1	0	0	0	0.0	0.0	0.0	-	40.0	40.0	40.0
Palestina	1	1	6019	5	2	1	1	0	0	0	0.0	0.0	0.0	0.0	33.3	33.3	33.3
Oman	1	0	309101	0	0	0	1	0	0	0	0.0	-	-	-	-	-	-
Yemen	1	0	452043	2	0	0	1	0	0	0	0.0	0.0	-	-	-	-	-
Niger	1	0	1183525	0	0	0	1	0	0	0	0.0	-	-	-	-	-	-
Mauritania	1	0	1040803	0	0	0	0	0	0	0	0.0	-	-	-	-	-	-
Eritrea	0	0	119719	0	0	0	0	0	0	0	0.0	-	-	-	-	-	-
Jordan	0	0	88670	9	11	5	0	0	0	0	0.0	0.0	0.0	0.0	0.0	0.0	0.0
United Arab Emirates	0	0	79190	0	0	0	0	0	0	0	0.0	-	-	-	-	-	-
Djibouti	0	0	21514	0	0	0	0	0	0	0	0.0	-	-	-	-	-	-
Saudi Arabia	0	0	1908357	0	0	0	0	0	0	0	0.0	-	-	-	-	-	-
Qatar	0	0	11214	0	0	0	0	0	0	0	0.0	-	-	-	-	-	-
Falkland Islands	0	0	11977	0	0	0	0	0	0	0	0.0	-	-	-	-	-	-
Kuwait	0	0	17384	0	0	0	0	0	0	0	0.0	-	-	-	-	-	-
Iceland	0	0	99299	0	0	0	0	0	0	0	0.0	-	-	-	-	-	-
Western Sahara	0	0	267282	0	0	0	0	0	0	0	0.0	-	-	-	-	-	-

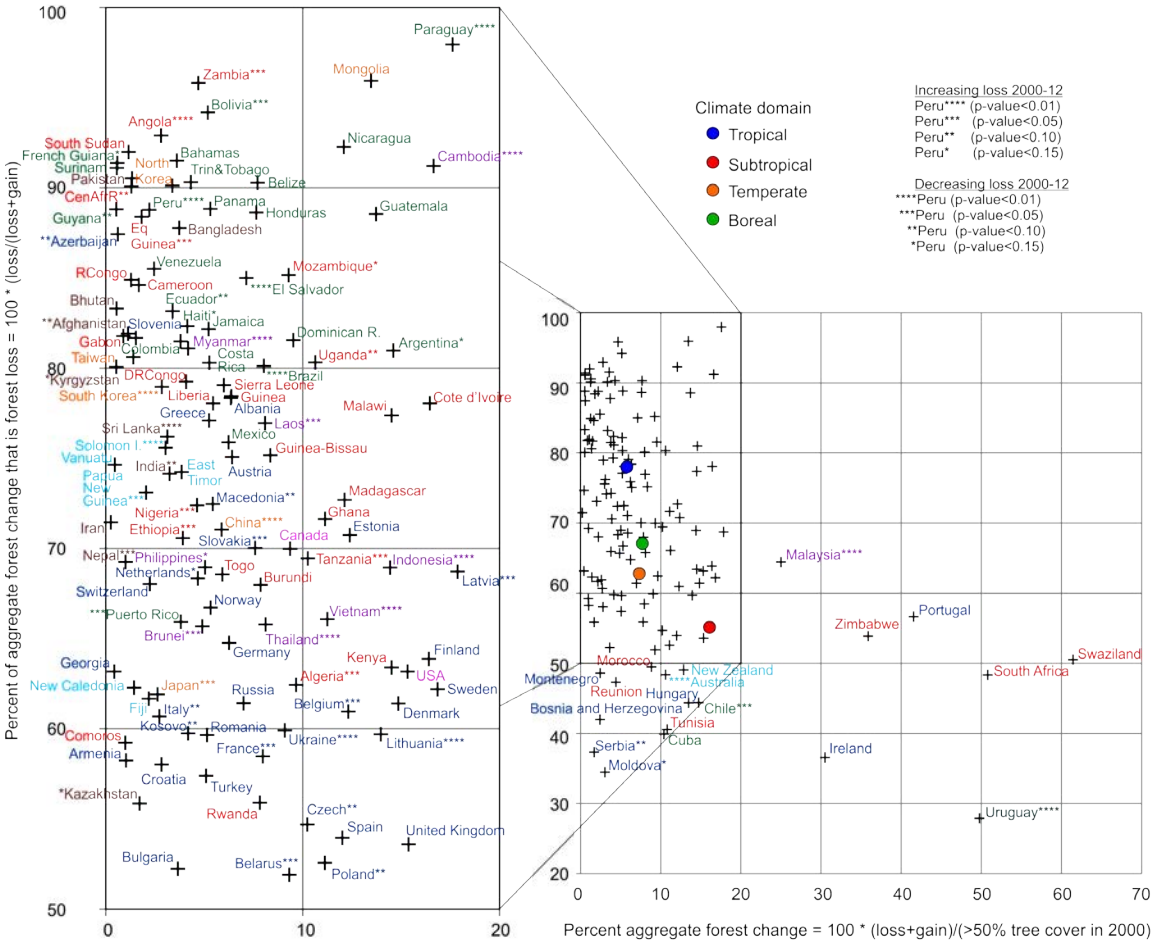

Fig. S1.

National and climate-domain scale intercomparisons using ratio measures of aggregate forest change ((loss+gain)/2000 forest) versus percent of aggregate forest change that is forest loss (loss/(loss+gain)). Countries exhibiting a statistically significant trend in forest loss during the study period are indicated (e.g. *** for p<0.05). Only countries with >1000km^2 of year 2000 >50% tree cover are shown. For this figure, forest is defined as tree cover >50%. Regional groupings are highlighted, with magenta= USA and Canada, green=Latin America, blue=Europe, red=Africa, brown=South Asia, purple=Southeast Asia, orange=East Asia, and cyan=Australia and Oceania. Refer to Tab. S1 and S3 for values.

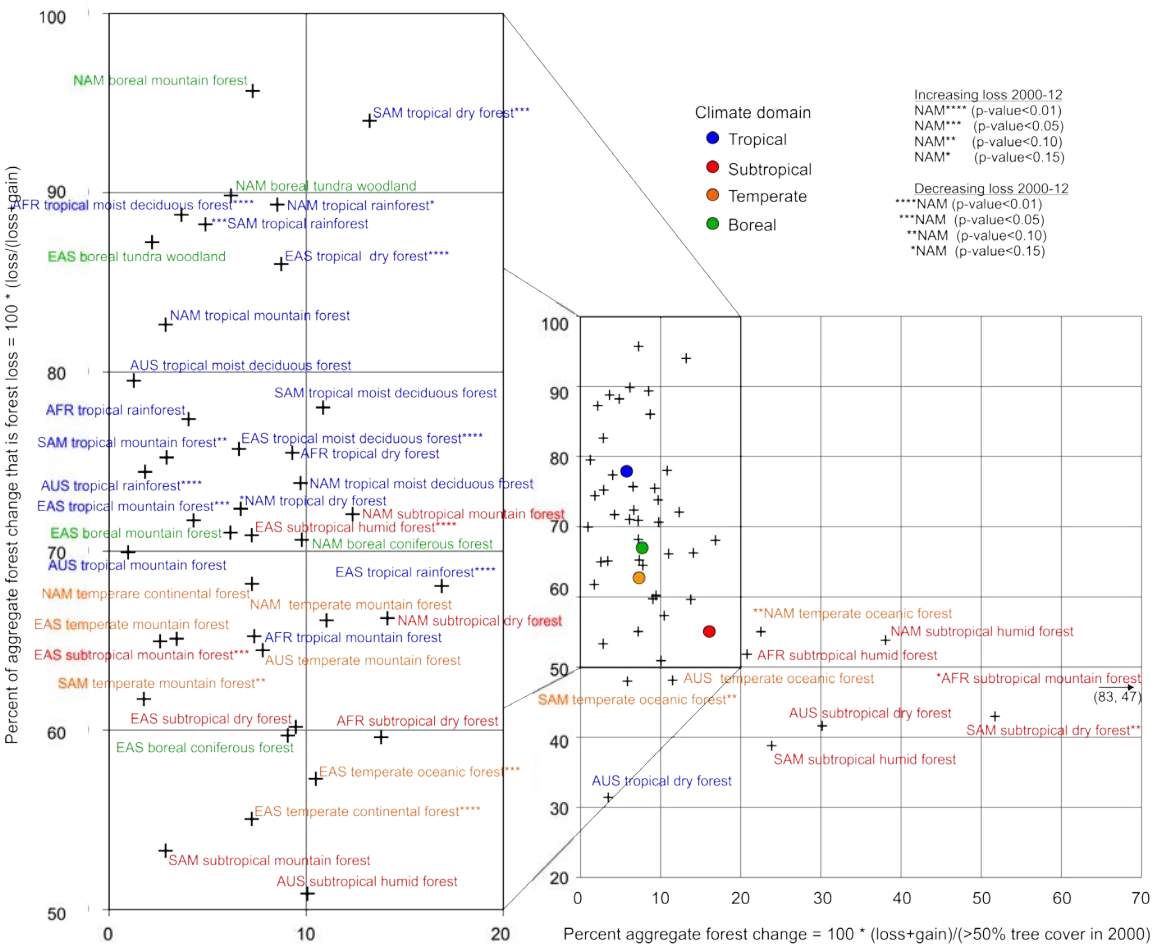

Fig. S2

Ecozone and climate-domain scale intercomparisons using ratio measures of aggregate forest change ((loss+gain)/2000 forest) versus percent of aggregate forest change that is forest loss (loss/(loss+gain)). Ecozones exhibiting a statistically significant trend in forest loss during the study period are indicated (e.g. *** for p<0.05). For this figure, forest is defined as tree cover >50%. Colors refer to climate domains; NAM=North America; SAM=South America; EAS=Eurasia; AFR=Africa; AUS=Australia and Oceania. Refer to Tab. S1 and S2 for values.

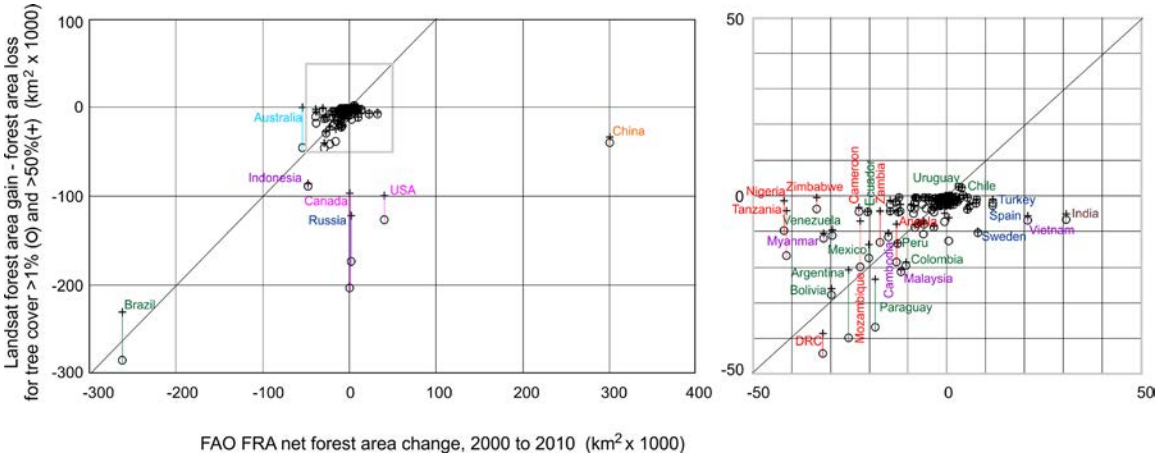

Fig. S3

FAO FRA net forest area change, 2000 to 2010, versus Landsat-derived net change, 2000 to 2012. Colors denote regional groupings of Fig. S2.

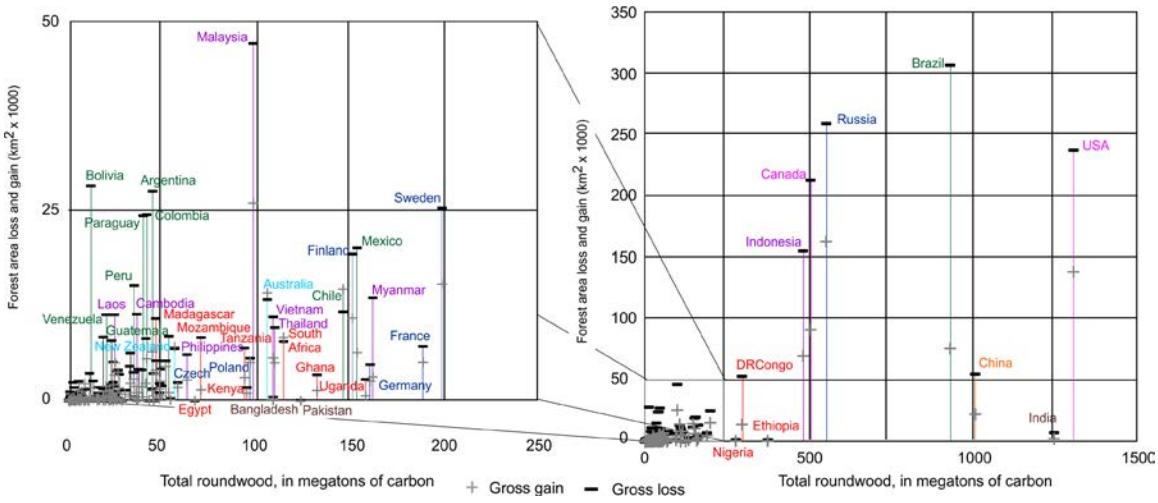

Fig. S4

FAO FRA roundwood production in megatons of carbon totaled per country from 2000 through 2011 versus total Landsat-derived forest area loss and gain from 2000 to 2012. Colors denote regional groupings of Fig. S2.

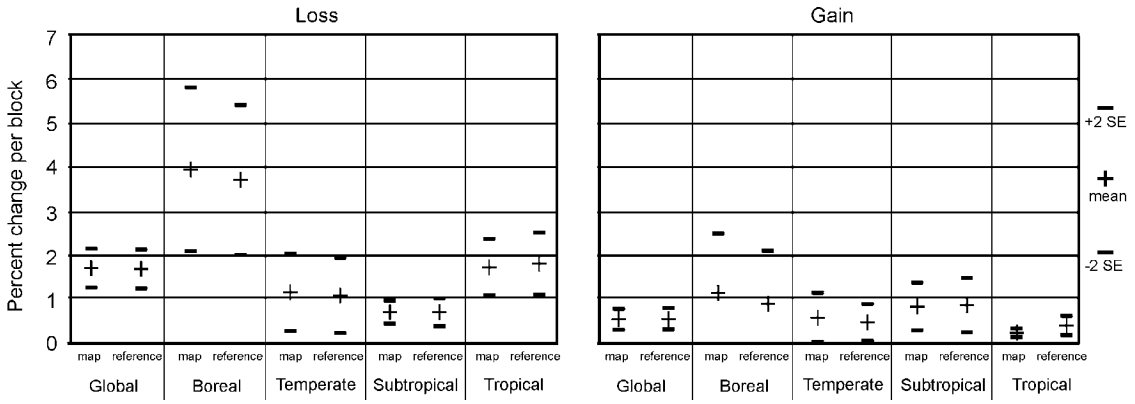

Fig. S5

Sample-based estimation of forest cover loss and gain, including all tree cover strata in loss estimation. Map is from the Landsat-derived map product. Reference is from validation data derived from multi-source image interpretation. Mean and two standard error range are shown at global and climate domain scales.

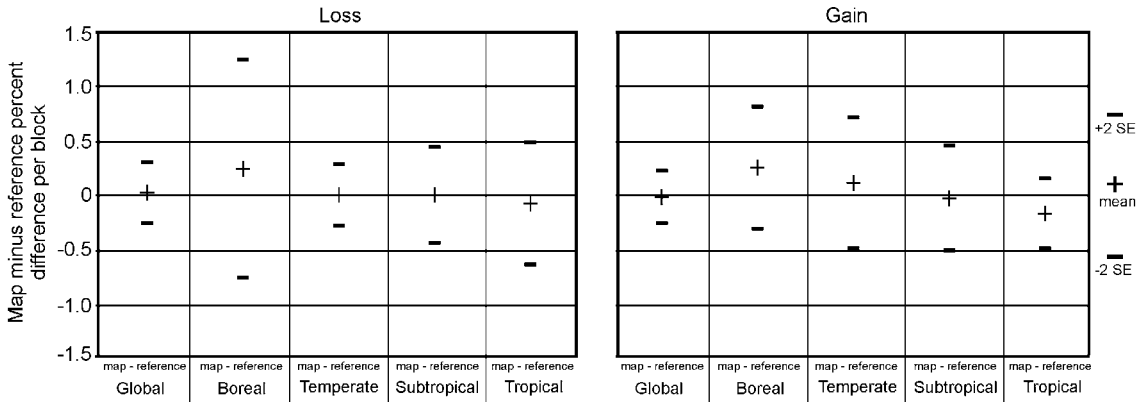

Fig. S6

Sample-based difference of map minus reference forest loss and gain per block, including all tree cover strata in loss estimation. Map is from the Landsat-derived map product. Reference is from validation data derived from multi-source image interpretation. Mean and two standard error range are shown at global and climate domain scales.

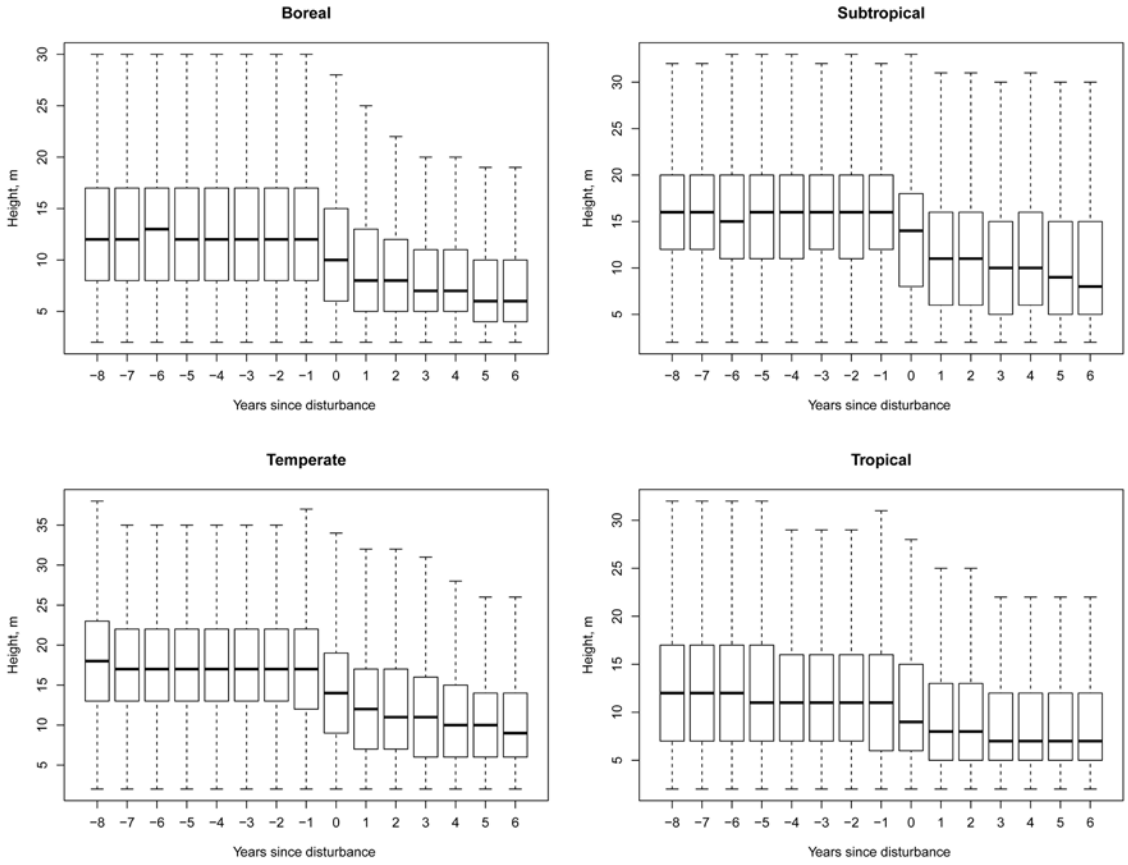

Fig. S7

GLAS-derived vegetation heights for Landsat-derived forest loss pixels. GLAS median and quartiles are displayed by number of years from Landsat-estimated year of disturbance.

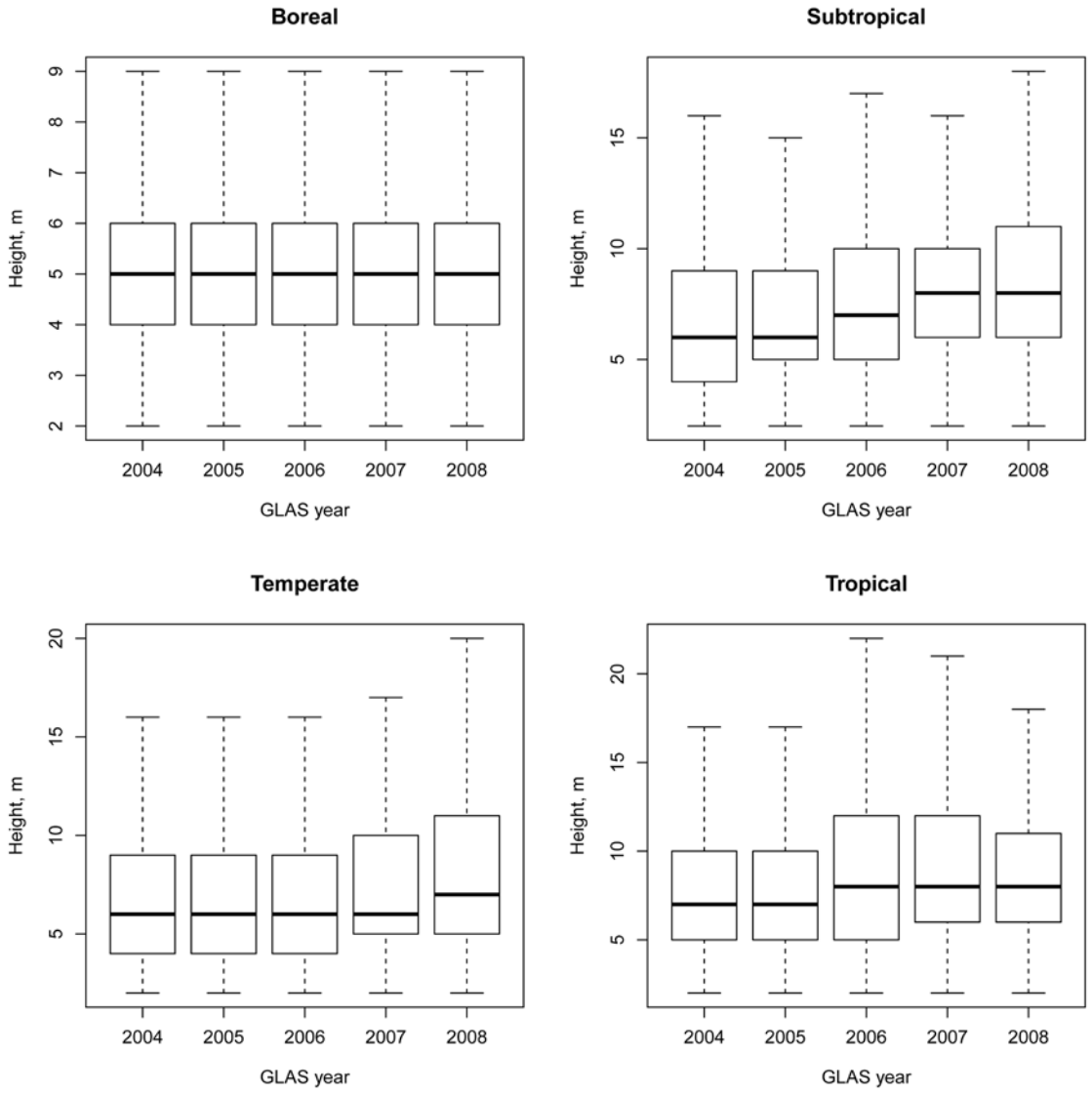

Fig. S8

Median and quartile GLAS-derived vegetation heights for areas of Landsat-derived zero percent tree cover in 2000 that were mapped as forest gain within the 2000 to 2012 study period.

Table S4.

Regression results for selected regions comparing 2000-2010 FAO FRA net change and 2000-2011 FAO roundwood production versus 2000-2012 global Landsat-derived gross forest area gain minus gross forest area loss for two tree cover thresholds (>1% and >50%).

Net area change	FRA vs. >1%		FRA vs. >50%	
	r^2	slope	r^2	slope
Latin America (excluding Brazil)	0.63	0.68	0.70	0.91
Africa (excluding DRC)	0.37	0.45	0.17	0.23
Southeast Asia (excluding Indonesia)	0.28	0.19	0.26	0.18
Europe (excluding Russia)	0.06	-0.16	0.02	-0.09

Roundwood production	FRA vs. gain area	FRA vs. loss area
	r^2	r^2
Latin America (excluding Brazil)	0.70	0.26
Africa (excluding DRC)	0.15	0.11
Southeast Asia (excluding Indonesia)	0.03	0.03
Europe (excluding Russia)	0.69	0.68

Table S5.

Accuracy assessment of 2000 to 2012 forest loss and gain at global and climate domain scales.

Global (n=1500)

Loss error matrix expressed as percent of area (selected standard errors are shown in parentheses)

		Reference			
		Loss	No Loss	Total	User's (SE)
Map	Loss	1.48	0.22	1.70	87.0 (2.8)
	No Loss	0.20	98.10	98.30	99.8 (0.1)
	Total	1.68	98.32		
	Producer's	87.8 (2.8)	99.8 (0.1%)		

Overall accuracy = 99.6% (0.7%)

Gain error matrix expressed as percent of area (selected standard errors are shown in parentheses)

		Reference			
		Gain	No Gain	Total	User's (SE)
Map	Gain	0.41	0.13	0.54	76.4 (0.6)
	No Gain	0.14	99.32	99.46	99.9 (0.0)
	Total	0.55	99.45		
	Producer's	73.9 (0.7)	99.9 (0.0)		

Overall accuracy = 99.7% (0.6%)

Climate domains

Tropical (n=628)

Loss error matrix expressed as percent of area (selected standard errors are shown in parentheses)

		Reference			
		Loss	No Loss	Total	User's (SE)
Map	Loss	1.50	0.22	1.72	87.0 (4.7)
	No Loss	0.30	97.98	98.28	99.7 (0.1)
	Total	1.80	98.20		
	Producer's	83.1 (5.3)	99.8 (0.1)		

Overall accuracy = 99.5 (0.1)

Gain error matrix expressed as percent of area (selected standard errors are shown in parentheses)

		Reference			
		Gain	No Gain	Total	User's (SE)
Map	Gain	0.19	0.04	0.23	81.9 (8.8)
	No Gain	0.21	99.56	99.77	99.8 (0.1)
	Total	0.40	99.60		
	Producer's	48.0 (8.6)	99.9 (0.1)		

Overall accuracy = 99.7 (0.1)

Subtropical (n=295)

Loss error matrix expressed as percent of area (selected standard errors are shown in parentheses)

		Reference			
		Loss	No Loss	Total	User's
Map	Loss	0.56	0.15	0.70	79.3 (8.6)
	No Loss	0.14	99.16	99.30	99.8 (0.1)
	Total	0.70	99.30		
	Producer's	79.4 (7.4)	99.8 (0.1)		

Overall accuracy = 99.7 (0.1)

Gain error matrix expressed as percent of area (selected standard errors are shown in parentheses)

		Reference			
		Gain	No Gain	Total	User's (SE)
Map	Gain	0.71	0.12	0.83	85.5 (8.9)
	No Gain	0.15	99.02	99.17	99.8 (0.1)
	Total	0.86	99.14		
	Producer's	82.4 (5.1)	99.9 (0.1)		

Overall accuracy = 99.7 (0.1)

Temperate (n=298)

Loss error matrix expressed as percent of area (selected standard errors are shown in parentheses)

		Reference			
		Loss	No Loss	Total	User's (SE)
Map	Loss	1.01	0.14	1.15	88.2 (5.4)
	No Loss	0.07	98.79	98.85	99.9 (0.1)
	Total	1.08	98.92		
	Producer's	93.9 (4.1)	99.9 (0.1)		

Overall accuracy = 99.8 (0.1)

Gain error matrix expressed as percent of area (selected standard errors are shown in parentheses)

		Reference			
		Gain	No Gain	Total	User's (SE)
Map	Gain	0.36	0.22	0.58	62.0 (15.0)
	No Gain	0.11	99.31	99.42	99.9 (0.1)
	Total	0.47	99.53		
	Producer's	76.5 (14.5)	99.8 (0.1)		

Overall accuracy = 99.7 (0.1)

Boreal (n=258)

Loss error matrix expressed as percent of area (selected standard errors are shown in parentheses)

		Reference			
		Loss	No Loss	Total	User's (SE)
Map	Loss	3.47	0.47	3.94	88.0 (4.7)
	No Loss	0.23	95.83	96.06	99.8 (0.1)
	Total	3.70	96.30		
	Producer's	93.9 (1.7)	99.5 (0.1)		

Overall accuracy = 99.3 (0.2)

Gain error matrix expressed as percent of area (selected standard errors are shown in parentheses)

		Reference			
		Gain	No Gain	Total	User's (SE)
Map	Gain	0.87	0.26	1.13	76.7 (11.8)
	No Gain	0.01	98.85	98.86	99.9 (0.1)
	Total	0.88	99.11		
	Producer's	98.4 (1.1)	99.7 (0.1)		

Overall accuracy = 99.7 (0.1)

References and Notes

1. J. A. Foley, R. Defries, G. P. Asner, C. Barford, G. Bonan, S. R. Carpenter, F. S. Chapin, M. T. Coe, G. C. Daily, H. K. Gibbs, J. H. Helkowski, T. Holloway, E. A. Howard, C. J. Kucharik, C. Monfreda, J. A. Patz, I. C. Prentice, N. Ramankutty, P. K. Snyder, Global consequences of land use. *Science* **309**, 570–574 (2005). doi:10.1126/science.1111772 Medline

2. M. C. Hansen, S. V. Stehman, P. V. Potapov, Quantification of global gross forest cover loss. *Proc. Natl. Acad. Sci. U.S.A.* **107**, 8650–8655 (2010). doi:10.1073/pnas.0912668107 Medline

3. Food and Agricultural Organization of the United Nations, *Global Forest Land-Use Change 1990-2005, FAO Forestry Paper No. 169* (Food and Agricultural Organization of the United Nations, Rome, 2012).

4. M. Hansen, R. DeFries, Detecting long-term global forest change using continuous fields of tree-cover maps from 8-km Advanced Very High Resolution Radiometer (AVHRR) data for the years 1982-1999. *Ecosystems (N. Y.)* **7**, 695–716 (2004). doi:10.1007/s10021-004-0243-3

5. Instituto Nacional de Pesquisas Especias, *Monitoring of the Brazilian Amazonian Forest by Satellite, 2000-2012* (Instituto Nacional de Pesquisas Especias, San Jose dos Campos, Brazil, 2013).

6. G. Sparovek, G. Berndes, A. G. O. P. Barretto, I. L. F. Klug, The revision of the Brazilian Forest Act: Increased deforestation or a historic leap towards balancing agricultural development and nature conservation. *Environ. Sci. Policy* **16**, 65–72 (2012). doi:10.1016/j.envsci.2011.10.008

7. D. P. Edwards, W. F. Laurance, Carbon emissions: Loophole in forest plan for Indonesia. *Nature* **477**, 33 (2011). doi:10.1038/477033a Medline

8. M. Drummond, T. Loveland, Land-use pressure and a transition to forest-cover loss in the Eastern United States. *Bioscience* **60**, 286–298 (2010). doi:10.1525/bio.2010.60.4.7

9. W. A. Kurz, C. C. Dymond, G. Stinson, G. J. Rampley, E. T. Neilson, A. L. Carroll, T. Ebata, L. Safranyik, Mountain pine beetle and forest carbon feedback to climate change. *Nature* **452**, 987–990 (2008). doi:10.1038/nature06777 Medline

10. B. Gardiner *et al*., *Destructive Storms in European Forests: Past and Forthcoming Impacts* (European Forest Institute, Freiburg, Germany, 2010).

11. P. Potapov, M. Hansen, S. Stehman, T. Loveland, K. Pittman, Combining MODIS and Landsat imagery to estimate and map boreal forest cover loss. *Remote Sens. Environ.* **112**, 3708–3719 (2008). doi:10.1016/j.rse.2008.05.006

12. A. Prishchepov, D. Muller, M. Dubinin, M. Baumann, V. Radeloff, Determinants of agricultural land abandonment in post-Soviet European Russia. *Land Use Policy* **30**, 873–884 (2013). doi:10.1016/j.landusepol.2012.06.011

13. United Nations Framework Convention on Climate Change, *Reducing Emissions from Deforestation in Developing Countries: Approaches to Stimulate Action – Draft*

Conclusions Proposed by the President (United Nations Framework Convention on Climate Change Secretariat, Bonn, Germany, 2005).

14. R. Houghton *et al*., The role of science in REDD. *Carbon Manage*. **1**, 253–259.

15. H. Geist, E. Lambin, Proximate causes and underlying driving forces of tropical deforestation. *Bioscience* **52**, 143–150 (2002). doi:10.1641/0006-3568(2002)052[0143:PCAUDF]2.0.CO;2

16. S. S. Saatchi, N. L. Harris, S. Brown, M. Lefsky, E. T. Mitchard, W. Salas, B. R. Zutta, W. Buermann, S. L. Lewis, S. Hagen, S. Petrova, L. White, M. Silman, A. Morel, Benchmark map of forest carbon stocks in tropical regions across three continents. *Proc. Natl. Acad. Sci. U.S.A.* **108**, 9899–9904 (2011). doi:10.1073/pnas.1019576108 Medline

17. A. Baccini, S. J. Goetz, W. S. Walker, N. T. Laporte, M. Sun, D. Sulla-Menashe, J. Hackler, P. S. A. Beck, R. Dubayah, M. A. Friedl, S. Samanta, R. A. Houghton, Estimated carbon dioxide emissions from tropical deforestation improved by carbon-density maps. *Nature Clim. Change* **2**, 182–185 (2012). doi:10.1038/nclimate1354

18. N. L. Harris, S. Brown, S. C. Hagen, S. S. Saatchi, S. Petrova, W. Salas, M. C. Hansen, P. V. Potapov, A. Lotsch, Baseline map of carbon emissions from deforestation in tropical regions. *Science* **336**, 1573–1576 (2012). doi:10.1126/science.1217962 Medline

19. R. Waterworth, G. Richards, C. Brack, D. Evans, A generalized hybrid process-empirical model for predicting plantation forest growth. *For. Ecol. Manage.* **238**, 231–243 (2007). doi:10.1016/j.foreco.2006.10.014

20. P. Potapov *et al*., Mapping the world's intact forest landscapes by remote sensing. *Ecol. Soc.* **13**, 51 (2008).

21. T. M. Brooks, R. A. Mittermeier, G. A. da Fonseca, J. Gerlach, M. Hoffmann, J. F. Lamoreux, C. G. Mittermeier, J. D. Pilgrim, A. S. Rodrigues, Global biodiversity conservation priorities. *Science* **313**, 58–61 (2006). doi:10.1126/science.1127609 Medline

22. A. S. Rodrigues, S. J. Andelman, M. I. Bakarr, L. Boitani, T. M. Brooks, R. M. Cowling, L. D. Fishpool, G. A. Da Fonseca, K. J. Gaston, M. Hoffmann, J. S. Long, P. A. Marquet, J. D. Pilgrim, R. L. Pressey, J. Schipper, W. Sechrest, S. N. Stuart, L. G. Underhill, R. W. Waller, M. E. Watts, X. Yan, Effectiveness of the global protected area network in representing species diversity. *Nature* **428**, 640–643 (2004). doi:10.1038/nature02422 Medline

23. T. Rudel, Is there a forest transition? Deforestation, reforestation and development. *Rural Sociol.* **63**, 533–552 (1998). doi:10.1111/j.1549-0831.1998.tb00691.x

24. G. P. Asner, D. E. Knapp, E. N. Broadbent, P. J. Oliveira, M. Keller, J. N. Silva, Selective logging in the Brazilian Amazon. *Science* **310**, 480–482 (2005). doi:10.1126/science.1118051 Medline

25. C. E. Woodcock, R. Allen, M. Anderson, A. Belward, R. Bindschadler, W. Cohen, F. Gao, S. N. Goward, D. Helder, E. Helmer, R. Nemani, L. Oreopoulos, J. Schott, P. S. Thenkabail, E. F. Vermote, J. Vogelmann, M. A. Wulder, R. Wynne, Free access to Landsat imagery. *Science* **320**, 1011 (2008). doi:10.1126/science.320.5879.1011a Medline

26. C. Tucker, D. Grant, J. Dykstra, NASA's orthorectified Landsat data set. *Photogramm. Eng. Remote Sensing* **70**, 313–322 (2004).

27. P. Potapov, S. A. Turubanova, M. C. Hansen, B. Adusei, M. Broich, A. Altstatt, L. Mane, C. O. Justice, Quantifying forest cover loss in Democratic Republic of the Congo, 2000-2010. *Remote Sens. Environ.* **122**, 106–116 (2012). doi:10.1016/j.rse.2011.08.027

28. M. Broich, M. C. Hansen, P. Potapov, B. Adusei, E. Lindquist, S. V. Stehman, Time-series analysis of multi-resolution optical imagery for quantifying forest cover loss in Sumatra and Kalimantan, Indonesia. *Int. J. Appl. Earth Obs* **13**, 277–291 (2011). doi:10.1016/j.jag.2010.11.004

29. M. Hansen, A. Egorov, D. P. Roy, P. Potapov, J. Ju, S. Turubanova, I. Kommareddy, T. R. Loveland, Continuous fields of land cover for the conterminous United States using Landsat data: First results from the Web-Enabled Landsat Data (WELD) project. *Remote Sens. Letters* **2**, 279–288 (2011). doi:10.1080/01431161.2010.519002

30. M. Hansen, R. S. DeFries, J. R. G. Townshend, M. Carroll, C. Dimiceli, R. A. Sohlberg, Global percent tree cover at a spatial resolution of 500 meters: First results of the MODIS vegetation continuous fields algorithm. *Earth Interact.* **7**, 1–15 (2003). doi:10.1175/1087-3562(2003)007<0001:GPTCAA>2.0.CO;2

31. L. Breiman, J. Friedman, R. Olsen, C. Stone, *Classification and Regression Trees* (Wadsworth and Brooks/Cole, Monterey, CA, 1984).

32. C. Chambers, A. Raniwala, F. Perry, S. Adams, R. R. Henry, R. Bradshaw, N. Weizenbaum, FlumeJava: Easy, efficient data-parallel pipelines. *ACM SIGPLAN Notices* **45**, 363–375 (2010). doi:10.1145/1809028.1806638

33. Food and Agricultural Organization of the United Nations, *Global Forest Resources Assessment* (Food and Agricultural Organization of the United Nations, Rome, 2010).

34. A. Grainger, Difficulties in tracking the long-term global trend in tropical forest area. *Proc. Natl. Acad. Sci. U.S.A.* **105**, 818–823 (2008). doi:10.1073/pnas.0703015105 Medline

35. F. Achard, H. D. Eva, H. J. Stibig, P. Mayaux, J. Gallego, T. Richards, J. P. Malingreau, Determination of deforestation rates of the world's humid tropical forests. *Science* **297**, 999–1002 (2002). doi:10.1126/science.1070656 Medline

36. P. Gong, J. Wang, L. Yu, Y. Zhao, Y. Zhao, L. Liang, Z. Niu, X. Huang, H. Fu, S. Liu, C. Li, X. Li, W. Fu, C. Liu, Y. Xu, X. Wang, Q. Cheng, L. Hu, W. Yao, H. Zhang, P. Zhu, Z. Zhao, H. Zhang, Y. Zheng, L. Ji, Y. Zhang, H. Chen, A. Yan, J. Guo, L. Yu, L. Wang, X. Liu, T. Shi, M. Zhu, Y. Chen, G. Yang, P. Tang, B. Xu, C. Giri, N. Clinton, Z. Zhu, J. Chen, J. Chen, Finer resolution observation and monitoring of global land cover: First mapping results with Landsat TM and ETM+ data. *Int. J. Remote Sens.* **34**, 2607–2654 (2013). doi:10.1080/01431161.2012.748992

37. J. Sexton *et al*., Global 30-m resolution continuous fields of tree cover: Landsat-based rescaling of MODIS Vegetation Continuous Fields with lidar-based estimates of error. *Int. J. Digit. Earth* **6**, 427–448 (2013).

38. G. Gutman, C. Huang, G. Chander, P. Noojipady, J. Masek, Assessment of the NASA-USGS Global Land Survey (GLS) datasets. *Remote Sens. Environ.* **134**, 249–265 (2013). doi:10.1016/j.rse.2013.02.026

39. M. Hansen, P. Potapov, S. Turubanova, in *Global Forest Monitoring from Earth Observation*, F. Achard, M. Hansen, Eds. (CRC Press, Boca Raton, FL, 2012), 93–109.

40. S. Goetz, R. Dubayah, Advances in remote sensing technology and implications for measuring and monitoring forest carbon stocks and change. *Carbon Manage.* **2**, 231–244 (2011). doi:10.4155/cmt.11.18